Contrast properties of reflective liquid crystal light valves in projection displays

by A. E. Rosenbluth D. B. Dove F. E. Doany R. N. Singh

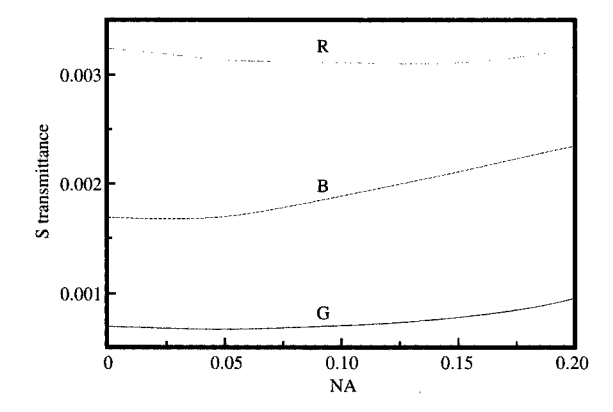
K. H. Yang M. Lu

Projectors that use reflective light valves must employ beam splitters or analogous components to separate bright-state light from dark-state light, since both states must propagate in the space above the light valve. Polarization ray tracing shows that such beam splitters will not usually achieve high rejection of dark-state light when the beam has the typical angular divergence of about ±10°. At such propagation angles, different rays in the beam will have appreciably different planes of incidence at tilted optical coatings in the system (because of the compound angles involved). If the light valve is mirrorlike in dark state, we show that to correct the depolarization resulting from compound incidence angles, it is necessary that the optics introduce no rotation in the illuminating polarization. To a reasonable approximation, such a rotation in polarization will double in the return pass through the optics. To the same approximation, induced

ellipticity in the illuminating polarization will cancel in double pass, and pure rotation can be converted to pure ellipticity with a quarterwave retarder. An important qualification, however, is that a light valve can only be exactly mirrorlike in restricted cases [i.e., if linearly polarized input light remains exactly linearly polarized (though possibly rotated) at all wavelengths when it reaches the mirror backplane of the light valve. independent of small manufacturing errors]. We calculate contrast loss in the more realistic case of a reflective twisted nematic liquid crystal (TNLC) light valve interacting with tilted coatings in the projection optics over finite numerical aperture (NA), and discuss the impact on LC thickness tolerances and spectral bandwidth $\Delta \lambda$. We extend our results to apply to more general light valves and more general projection optics configurations. Darkstate background is found to scale as NA² (or

©Copyright 1998 by International Business Machines Corporation. Copying in printed form for private use is permitted without payment of royalty provided that (1) each reproduction is done without alteration and (2) the Journal reference and IBM copyright notice are included on the first page. The title and abstract, but no other portions, of this paper may be copied or distributed royalty free without further permission by computer-based and other information-service systems. Permission to republish any other portion of this paper must be obtained from the Editor.

0018-8646/98/\$5.00 © 1998 IBM



Flaure

Measured S transmittance of commercially procured beam-splitter coating. R, G, and B refer to integrations over the red, green, and blue regions of the spectrum. A typical requirement of 100:1 system contrast can be met without a supplementary polarizer in the transmission path.

in some cases as ${}^{\sim}NA^2\Delta\lambda^2$). Because of this interaction, the complete system almost always shows a lower contrast than the light valve alone.

Introduction

Light valves that are reflective provide important advantages in projection displays. Controlling circuitry placed below the mirror surface does not obstruct the clear aperture [1, 2], more advanced IC technology is available for substrate materials that are opaque, and a more compact system may be achieved when the reflected output beam is folded back on the input. However, complexities arise in the optical system when the space above the light valve must be used for both illumination and collection. The reversibility of a nominally loss-free optical system implies that the light valve must be illuminated with dark-state light, because light that remains in the input state after reflecting from the light valve necessarily follows the reverse path back to the illuminator, and so does not contribute to image brightness. In different technologies the term dark-state might refer either to the polarization or to the directionality of the incident light, depending on the method of modulation used. In either case, it is a basic physical requirement that any light which the light valve might reflect without modification (in polarization or direction) will necessarily retrace its path back to the source.

Conversely light that is switched to the bright state by the light valve must be shunted into the projection optics. When light valves use polarization modulation, this is generally accomplished with a polarizing beam splitter (PBS), but the required angular range can be difficult to achieve. For one thing, it can be difficult to achieve acceptable performance from the polarizing hypotenuse coating over an adequate angular range (e.g., over a range of angles of incidence $\sim 45^{\circ} \pm 5^{\circ}$ in glass).

There is, however, a more subtle problem, relating to the difficulty in maintaining a consistent polarization in a three-dimensional cone of light as it propagates through an optical system. The angular subtense required in the beam [essentially, the numerical aperture (NA) or f/#] is dictated by the need for high lumen output, often the paramount requirement in today's projection displays. Typical output requirements and efficiency constraints imply optical fluxes at the light valve of ~ 1 W. Integratedcircuit processing techniques typically constrain the aperture of reflective light valves to dimensions of a few centimeters or less. Brightness limits in today's short-arc lamps then imply that the beam illuminating the light valve must subtend at least several degrees in order to provide the necessary flux density [3]. Polarization control with twisted nematic liquid crystal (TNLC) light valves and PBS optics over such angular ranges are the main emphasis of this paper. However, it is worth noting that the problem of preventing "crosstalk" between bright-state and dark-state beams is fairly general with reflective light valves, affecting, for example, those based on directional modulation.

Broadband polarizing beam splitters have been procured commercially that provide dark-state rejection >250:1 throughout the visible spectrum if used single-pass at any angle within a $\pm 10^{\circ}$ range. (A supplementary sheet polarizer must be included when the PBS is used in reflection.) Figures 1 and 2 illustrate the coating performance achieved. Imperfect coating response was distinguished from substrate birefringence in the measurements in Figures 1 and 2 by crossing the PBS pass direction against parallel input and output sheet polarizers. Measurements with a solid cube were used to subtract out losses in the prism substrates and front-surface antireflection coatings. Some PBS substrate glasses introduce appreciable attenuation in the blue region of the spectrum, but blue losses in the substrates of Figures 1 and 2 were small compared to those arising in other parts of the system, e.g. from illuminator components and aluminum fold mirrors [3]. The plotted results are integrated over a uniform cone of rays at each NA. It should be noted that while this coating provides reasonably high efficiency out to $NA \sim 0.2$, the design range was only $\pm 6^{\circ}$.

¹ For example, Balzers Thin Films Products Division, Fremont, CA; Spectra-Physics Components and Accessories Division, Mountain View, CA.

In a projector the PBS must be used in both transmission and reflection. One mode (e.g., transmission) is used for the illumination pass to the light valve, and the other (e.g., reflection) for collection from the light valve by the projection lens. MacNeille-type PBS coatings are designed to be dielectric mirrors in S polarization; a far more difficult requirement in their design is that they achieve Brewster suppression of P reflectivity throughout the ~±10° angular range. In practice, achieved P transmittance always departs much further from the goal of 100% than does S reflectance, so P transmittance gates double-pass PBS efficiency. Total background light in projection displays must typically be ≤1 part in 100 of bright state; the departure of P transmittance from unity is inevitably larger than this, which means that a supplementary polarizer (e.g., a sheet polarizer) must be included in the reflection pass to block reflected P light (i.e., if the light valve is illuminated with light reflected from the PBS hypotenuse, the illumination must be passed through a sheet polarizer before entering the PBS; if instead the image light is collected in reflection, the image light must be passed through a sheet polarizer after reflecting from the PBS). Sheet polarizers are at best ~90% efficient in the pass polarization, and it is desirable that the S transmittance be low enough that one does not have to add a second lossy sheet polarizer for the transmission arm. (Note that such a sheet polarizer in the illuminator might be replaced by more expensive polarizing elements that partially recycle the unused polarization [3-5].) Figures 1 and 2 show that coatings available today can achieve these performance goals; single-pass reflectance of P polarization and single-pass transmission of S polarization are both acceptably low by the above criteria.

However, basic trigonometric constraints limit the rejection ratio that can be achieved by the PBS element in double-pass, if it is used to illuminate a reflective substrate with a noncollimated beam. If the light valve returns dark-state light in mirrorlike fashion, the geometry of compound angles implies that skew rays will not see the same plane of incidence at the return pass to the PBS hypotenuse that they see on the input pass.

For skew rays these planes of incidence are tilted relative to the external faces of the PBS cube. For example, Figure 3 shows a skew ray AB incident at the front face of a PBS cube; the ray illuminates the light valve at point C after being reflected downward from point B by the hypotenuse coating. If the light valve is switched dark, the ray remains (nominally) dark-state polarized, and returns to the front face along CB'A'. During the input pass the PBS will polarize the illumination either perpendicular to the tilted plane of incidence ABC (for illumination in reflection through the PBS, as shown in Figure 3), or within this tilted incidence

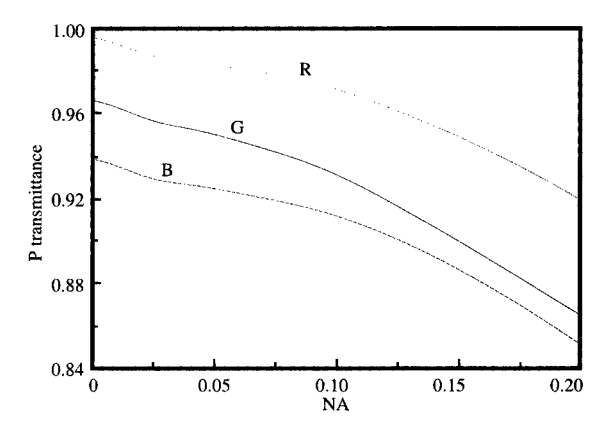


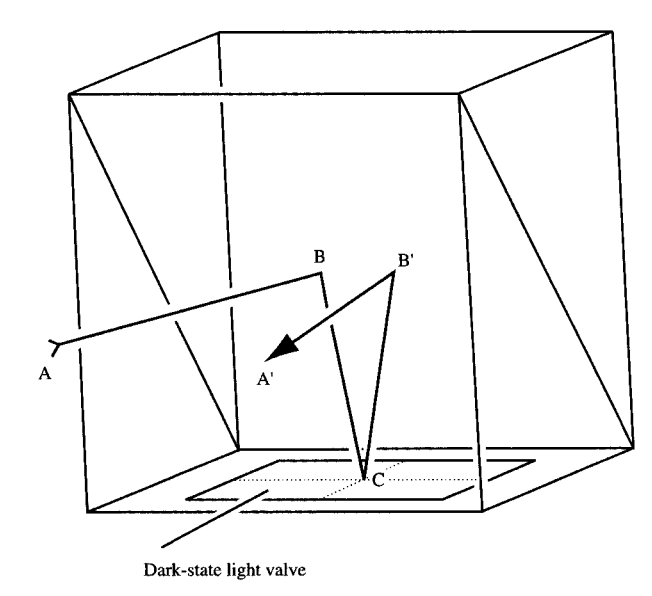
Figure 2

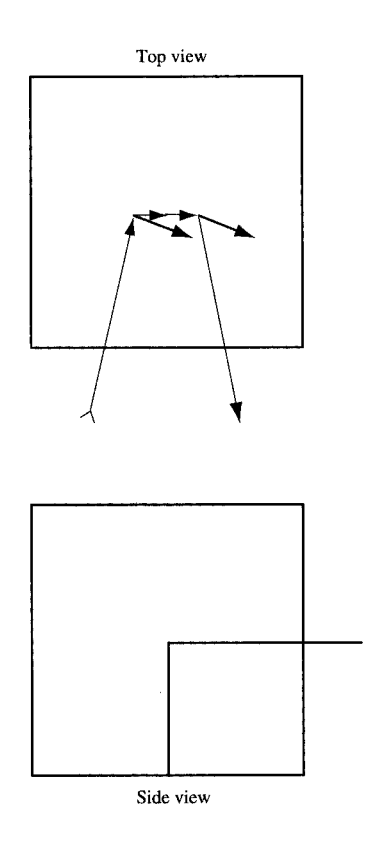
Measured P transmittance of the Figure 1 polarizing coating. At practical NAs, several percent of the light is lost in reflection. A supplementary polarizer in the reflection arm is required to meet typical contrast requirements; this entails $\gtrsim 10\%$ additional loss in throughput if an absorbing sheet polarizer is used.

plane (for illumination in transmission, not shown in Figure 3). If the illumination polarization is maintained in the dark-state light that reflects from the light valve, the *E*-field will show a different tilt relative to the new plane of incidence for the return pass at the PBS hypotenuse (plane A'B'C). The top-view diagram of Figure 3 illustrates the incident and returned *E*-field for the case of a light valve with mirrorlike dark state. The returned skew ray is reflected to the opposite side of the lens NA, causing the return plane of incidence A'B'C to have an opposite tilt from the input incidence plane ABC. The newly tilted orientation of the *E*-field relative to A'B'C means that the dark-state light has both S and P components during the return pass, and so is not entirely returned to the illuminator.

By this mechanism, the compounded incidence angle of the ray at the PBS coating (the ray incidence angle having components along both the skew and coating-tilt meridians) gives rise to polarization crosstalk, causing a loss in contrast. The amplitude projection onto the tilted incidence plane is approximately linear with NA, and contrast decreases as NA^{-2} . Since compound-angle depolarization converts dark-state light to the bright state of the image, this NA-dependent background cannot be filtered out with a supplementary polarizer.

This depolarization mechanism does not ordinarily arise with transmissive light valves, where a simple sheet post-polarizer can be used to trim dark-state light from the bright-state image beam. When the light valve is reflective, both states must propagate in the space above the





Rays are incident at beam splitter with appreciable skew angle when optical system aperture provides acceptable brightness ($NA \gtrsim 0.1$). The compound incidence angles cause polarization crosstalk that is proportional to the varying tilt in the ray planes of incidence (e.g., ABC, A'B'C). The resulting loss in contrast cannot be corrected with a supplementary polarizer. Note: For the sake of clarity, refraction at the front surface is not shown.

substrate, and the beam-splitter element must actually separate the two beams. Beam-dividing interference coatings are prone to the depolarization mechanism described above. A transmission light valve will not suffer compound-angle depolarization even when PBS pre- and post-polarizers are used instead of sheet polarizers, as long as the hypotenuse coatings of the two PBS cubes are parallel and there are no other tilted coatings between the PBSs and the light valve. However, single-pass compoundangle effects are reported [6] in rear-projection monitors that reduce box depth by using a reflective polarizer [7, 8] on the inside surface of the projection screen in order to make an extra fold in the imaging beam [6, 9].

As discussed above, the ideal reflective light valve must, when switched to dark-state, reflect the central ray without changing its polarization. However, such an ideal light valve need not be mirrorlike; it might, for example, be instead equivalent to a quarter-wave retarder placed above

a mirror. As long as the fast and slow axes of such a retarder take the orientation shown by the dashed lines in Figure 3 (one axis lying within the plane BB'C, the other axis parallel to the central ray before it enters the cube), the dark-state polarization of the input central ray will remain unchanged in the output. However, such a quarter-wave retarder will change the polarization of skew rays, in a beneficial way. The retarder will act as a half-wave rotator in double pass, and the E-field of a skew ray that is incident perpendicular to (or within) the rotated plane ABC will be returned in a direction perpendicular to (or within) the mirror-rotated plane A'B'C, thereby eliminating depolarization [10]. If the dark-state light valve resembles a mirror rather than a quarter-wave plate, the same correction can of course be obtained by placing an actual quarter-wave retarder above the light valve. This technique appears to be fairly well known among manufacturers of light-valve projectors

(perhaps having been invented independently a number of times), but to our knowledge it has only been described in the patent literature [10].

In this paper we describe the above depolarization mechanism in more general terms; we consider more general optical systems than the simple PBS of Figure 3, and we consider light valves that are not necessarily ideal. We do, however, make the following approximation: In cases where the central ray strikes a surface at (or near) normal incidence, we apply the normal-incidence Jones matrix for the surface to all rays in the beam. (In fact, it is only in this approximation that one can describe the E-field reflected from a mirror as not rotated.) Terms that scale as NA^2 (in amplitude) are thereby neglected. However, we show that tilted optical coatings in the system give rise to amplitude effects that scale as NA¹ (as in the example of Figure 3); these linear terms are dominant. Comparison with exact-polarization ray tracing shows that a first-order calculation predicts background levels to well below one part in 100 at NAs of interest to us, i.e., at apertures below $\sim f/3.5$ (NA $\lesssim 0.14$). (When we use the term first-order in this work without further qualification, we mean first-order in an expansion in beam NA.) More accurate calculations require modeling of the angular dependence of near-normal incidence components such as linear sheet polarizers and the light valve; these are beyond the scope of the present paper. However, we note that the mechanics of exact-polarization ray tracing are well known in the literature, and are implemented in commercial optical design programs. Most commonly, polarization along a ray is determined from a multiplied string of Jones matrices, alternating between matrices for the surfaces and matrices that carry out rotation transforms to map the S and P polarization directions of one surface to the S and P directions for the next. To our knowledge, the first such treatment to use a modern ray-tracing formulation is that of Waluschka [11]; full implementation details are given in his paper. Waluschka's method is useful for calculating the polarization properties of projection optics at a system level. The polarization properties of LC light valves are described in two recent reviews [12, 13].

A first-order calculation is sufficiently accurate for our purposes, and the simplification it provides yields two advantages. First, such a calculation allows contrast to be defined in terms of simple relationships involving surface parameters (usually, the surface orientations and the S/P relative phase shifts from interference coatings on the surfaces). Simple relationships are particularly advantageous in an optimization program, where rapid evaluation of a merit function is important.

Second, a first-order analysis provides considerable insight into the nature of contrast loss from interaction between the optics and the light valve. This is the main

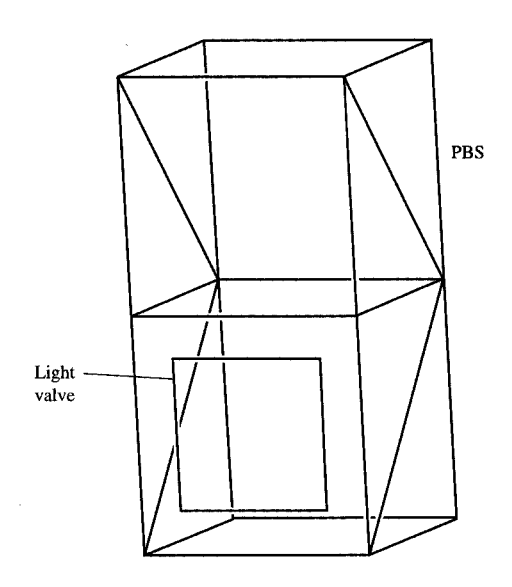


Figure 4 Compound-angle depolarization can arise as a cumulative effect from multiple tilted coatings in the optical system.

emphasis of the present paper. Contrast with a general optical system and light valve is found to scale as NA^{-2} under the compound-angle depolarization mechanism. The analysis below shows that a succession of optical surfaces that are parallel to the PBS hypotenuse (in media having roughly similar refractive indices) do not give rise to further depolarization. Only surfaces where bright-state and dark-state light propagate together give rise to relevant depolarization; as illustrated in Figure 4, these might include color-splitting dichroics between the PBS and the light valves. Only bright-state light propagates between the PBS and the projection lens, but dark-state and bright-state light must both propagate through surfaces that lie between the PBS and the light valve, and dark-state light traverses these surfaces in double pass. This double-pass traversal implies a degree of symmetry in the depolarization properties; we show that when the dark-state light valve can be approximated as mirrorlike, rotation imposed on the illuminating polarization by the optics during the input pass is essentially doubled during the output pass, and ellipticity is canceled. This is opposite to the usual symmetry in double-pass traversal of a polarizing element, where (for small depolarization) ellipticity doubles and rotation is canceled (as with a waveplate or optically active film above a mirror); the difference is that a skew ray propagates through the optics on opposite sides of the pupil during the input and output passes.

Note that what is meant here by "doubling of rotational depolarization in round trip" is that when the single-pass depolarization of skew rays is purely rotational (i.e., E_x/E_z is pure real at the completion of a single pass through the optics when the input ray cone is linearly polarized along \hat{z} , with optical axis along \hat{y}), the double-pass depolarization will be twice as large in magnitude. The double-pass intensity between crossed polarizers is then four times that measured in single pass if the single-pass depolarization is purely rotational. However, while the depolarization doubles in magnitude after two passes, the direction of polarization in the beam that exits the system is always aligned with the PBS pass axis for the bright-state image, which is oriented at approximately 90° to the polarization that illuminates the light valve.

It is not necessary that the light valve be mirrorlike in dark state to provide high contrast. We later show [Equation (64)] that when any continuous polarizationmodulating layer is placed above a mirror backplane and rotated between crossed polarizers, the reflectance (in double-pass traversal of the layer) will be proportional to $\sin^2(2\Theta')$, with Θ' the orientation (measured relative to the orientation of minimum reflectivity), as long as the layer is not lossy from scattering or absorption. One must imagine that the beam is incident on the reflecting structure at an angle slightly off normal, so that the input and output polarizers can be crossed to each other. The amplitude of the $\sin^2(2\Theta')$ variation is only zero (for all Θ') if the polarization-modulating layer (in single pass) is either null, equivalent to a half-wave retarder, or equivalent to a pure rotation (optically active layer). On the other hand, a PBS in a projector functions "in zeroth order" (i.e., $NA \rightarrow 0$) as crossed polarizers, so to zeroth order essentially any polarization-modulating film above a mirror can be said to provide a valid dark state if rotated to a particular orientation where the $\sin^2(2\Theta')$ modulation has a zero. (Of course, in practice a light-valve active layer must in dark state be reasonably insensitive to depolarization from scatter and small inhomogeneities, it must satisfy spectral bandwidth requirements, and it must provide adequate performance when $NA \neq 0$.)

If the light valve is not mirrorlike, we still find that when $NA \neq 0$, one portion of the single-pass depolarization from the optical system will be canceled in the return pass, and the remaining portion will double (in amplitude). As noted above, depolarization refers to the complex electric field amplitude that is output with polarization in the orthogonal state to a linear polarized input, divided by the output in the parallel polarization. We show that the relationship between single-pass and double-pass contrast loss can be expressed very simply in terms of the phases of the light valve and optics depolarizations. For this reason it is convenient to analyze the projection properties of the system by propagating a

single complex scalar (namely the depolarization) from surface to surface, rather than by propagating a Jones vector. However, we follow the Jones-matrix approach of Lu and Saleh [14] in analyzing the light valve.²

If a reflective light valve comprises an active polarizing layer [polarizing in the general sense of altering the polarization, e.g., a twisted nematic liquid crystal (TNLC) layer] above a bottom reflecting surface, we would expect that the conventional reversal symmetry would apply to the active layer itself. In that case, if control of the thickness of the polarizing layer is imperfect, and/or the light valve is to be used over an appreciable spectral bandwidth, we can only expect ideal contrast from the light valve in a simple crossed-polarizer measurement if the E-field within the active layer is linear at all depths close to the bottom mirror (since the exact depth of the mirror may vary), and is so linear at all wavelengths of interest. The light-valve active layer might cause the E-field at the bottom mirror to be rotated, but with the conventional reversal symmetry such rotation is canceled in the return pass through the layer. However, when the active layer produces ellipticity in the light illuminating the mirror backplane, this single-pass depolarization is not canceled in the return pass. When the single-pass depolarization is small (small rotation and small ellipticity), the elliptical component of the depolarization doubles in the return pass (in the sense that the intensity between crossed polarizers is approximately quadruple that of a transmission cell with an active layer producing the same single-pass ellipticity), causing the dark-state illumination to be partially converted to bright-state. [These results are derived below in Equation (49).] Thus, the optimum behavior for the light valve in the "zerothorder" case where the optics is ignored is that it produce no ellipticity at any wavelength in the light illuminating the mirror backplane, despite the presence of possible variations in layer thickness. (Note that skew-angle depolarization in the optics thus obeys a symmetry opposite to that of the light valve.) Unfortunately, the absence of ellipticity at all depths and wavelengths is difficult to achieve in a medium that shows both birefringence and a twist, as with TNLC. [An exception is a TNLC operating in the Maugin limit ([16]; see also [17, 18]); this case, however, is usually not practical for reflection light valves.] Thus, it is not surprising that, as shown below, a dark-state TN light valve of given thickness typically exhibits truly mirrorlike behavior at only a single wavelength in the operating spectral range. Even at this unique wavelength, we show that polarization rotation by the optics (but not imposed ellipticity)

 $^{^2}$ References pointed out by an anonymous reviewer brought to our attention the work of Ong [15], who analyzed LC light valves in terms of the depolarization (denoted χ by Ong), rather than Jones matrices. It might have been easier to integrate our optics model with Ong's light-valve formalism instead of the matrix-based approach of Reference [14].

gives rise to dark-state background $\propto NA^2$. At other wavelengths, the light valve interacts with both ellipticity and rotation imposed by the optics, again with scaling $\propto NA^2$ or $\propto NA^2\Delta\lambda^2$, where $\Delta\lambda$ is the shift away from the optimal wavelength. If the TN light valve is used between simple crossed polarizers $(NA \rightarrow 0)$, background is found to scale $\propto \Delta\lambda^4$; such quartic contributions are also present when the light valve is used in an optical system $(NA \neq 0)$.

Analysis

Light valve

The Jones matrix of a dark-state TN light valve has been derived by Lu and Saleh [14]. We use their formulation and notation, except we correct for what we believe is a sign error in their result. (This is above and beyond the difference between their sign convention and the sign convention used here.) The sign error appears to have propagated into their expression from a result of Yariv and Yeh [19]; since this result is widely cited in the literature, we sketch out the derivation here. Matrix element signs would not usually matter in a simple crossed-polarizer measurement of light-valve contrast, but can be important in analyzing the interaction with an optical system.

Figure 5 shows schematically the n_c axis twisting from top to bottom of an LC layer, with α the total twist angle. (In Figure 5 α is +45°.) We use (E_x, E_z) as the Jones vector, and use the sign convention where waves oscillate as $\exp \left[+iky - i\omega t \right]$. Following Yariv and Yeh [19], we introduce a rotating coordinate system that tracks the twisting LC molecules; we then write the single-pass Jones matrix M_{LC} for the LC layer in dark state as the result of propagation through a large number N of birefringent slabs with progressively twisting orientation:

$$\mathbf{M}_{LC} = \lim_{N \to \infty} \mathbf{R} \left(\alpha \, \frac{N-1}{N} \right) \left[\Delta \mathbf{M} \, \mathbf{R} \left(-\frac{\alpha}{N} \right) \right]^{N-1} \Delta \mathbf{M}, \tag{1}$$

where ΔM and $R(\theta)$ are respectively defined as

$$\Delta \mathbf{M} = \begin{pmatrix} e^{i(\beta/N)} & 0 \\ 0 & e^{-i(\beta/N)} \end{pmatrix} \quad \text{and} \quad \mathbf{R}(\theta) = \begin{pmatrix} \cos \theta & -\sin \theta \\ \sin \theta & \cos \theta \end{pmatrix}. \tag{2}$$

Here β is one half the integrated birefringence across the thickness d of the LC layer; $\beta = \pi(n_c - n_o)d/\lambda$ $[n_c]$ and n_o are the indices of refraction for the extraordinary and ordinary rays, respectively; they apply for the particular y-tilt of the LC molecule (assumed not to vary with depth y when the light valve is in dark state)].

One way to evaluate the matrix exponential in Equation (1) is to use a generalized DeMoivre identity [20]:

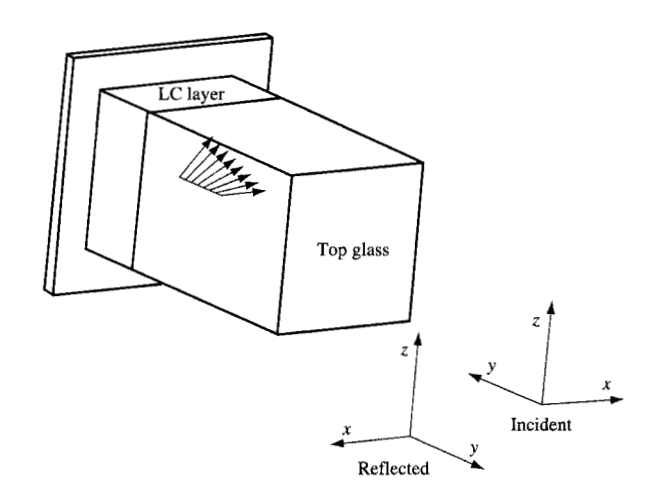


Figure 5

Sign convention for Jones matrices. A positive liquid crystal twist angle is illustrated ($\alpha = +45^{\circ}$).

$$(I\cos(\omega) + i\hat{n} \cdot \bar{\sigma} \sin(\omega))^m = (e^{i\omega\hat{n}\cdot\bar{\sigma}})^m = e^{im\omega\hat{n}\cdot\bar{\sigma}}$$
$$= I\cos(m\omega) + i\hat{n} \cdot \bar{\sigma} \sin(m\omega),$$
(3)

where I is the identity matrix and $\bar{\sigma}$ is a length-3 operator whose x, y, z components are the 2 \times 2 Pauli matrices σ_x , σ_y , and σ_z :

$$\sigma_{x} \equiv \begin{pmatrix} 0 & 1 \\ 1 & 0 \end{pmatrix}, \quad \sigma_{y} \equiv \begin{pmatrix} 0 & -i \\ i & 0 \end{pmatrix}, \quad \sigma_{z} \equiv \begin{pmatrix} 1 & 0 \\ 0 & -1 \end{pmatrix}, \quad (4)$$

and where \hat{n} is an arbitrary unit vector.

Applying Equation (4) to Equation (1) and then applying Equation (3), we obtain almost by inspection the following very compact expression for the single-pass Jones matrix of a TNLC layer with zero applied voltage:

$$\mathbf{M}_{LC} = e^{-i\alpha\sigma_{\mathbf{y}}} e^{i(\alpha\sigma_{\mathbf{y}} + \beta\sigma_{\mathbf{z}})}.$$
 (5)

(Note that the exponents cannot simply be added because the matrices do not commute.) Using Equation (3) to cast Equation (5) into more familiar notation, we obtain the well-known result, appearing here with consistent signs:

$$\mathbf{M}_{LC} = \mathbf{R}(\alpha) \begin{pmatrix} \cos \gamma + i\beta \frac{\sin \gamma}{\gamma} & \alpha \frac{\sin \gamma}{\gamma} \\ -\alpha \frac{\sin \gamma}{\gamma} & \cos \gamma - i\beta \frac{\sin \gamma}{\gamma} \end{pmatrix}, \tag{6}$$

where $\gamma = \sqrt{\alpha^2 + \beta^2}$. We believe that Equation (6) shares its consistency in signs with results in, e.g., Reference [21], but not with, e.g., References [14, 19]. Note that a common phase factor is neglected in Equation (6).

To determine the double-pass matrix of the light valve, denoted M_{LV} , we must specify further details of our sign convention. In most of this paper we use the sign convention recently reviewed by Pistoni [22], in which, for Jones vector (E_x, E_z) , the x-axis unit vector is assumed to reverse direction in space after a normal-incidence reflection from a surface, while \hat{z} remains unchanged; \hat{y} is taken to point in the direction of travel of the ray, and so of course reverses direction also. In this convention, \hat{x} , \hat{y} , \hat{z} remains a right-handed triad after reflection. Unfortunately, this conflicts with the most common sign convention in thin-film coating design, where it is most often considered preferable that the S and P reflectivities converge to the same value at normal incidence.

In the right-hand-preserving convention, the matrix for the reversed path through a (lossless) element can be obtained very quickly from the matrix for the initial direction of propagation. Specifically, if M^(rev) denotes the reverse-path matrix, we have [22]

$$\mathbf{M}^{\text{(rev)}} = \begin{pmatrix} m_{11} & -m_{21} \\ -m_{12} & m_{22} \end{pmatrix}, \tag{7a}$$

where the forward matrix is

$$\mathbf{M} = \begin{pmatrix} m_{11} & m_{12} \\ m_{21} & m_{22} \end{pmatrix} . \tag{7b}$$

Note that for our purposes only differential phases between S- and P-polarized components are important; absolute phase factors can be dropped. Similarly, Equation (7) will usually apply to a lossy element if the losses are equal in S and P polarizations. For such elements there are other symmetries we can exploit; for example, it is well known that their Jones matrices can always be expressed in such forms as

$$\mathbf{M} = \begin{pmatrix} m_{11} & m_{12} \\ -m_{12}^* & m_{11}^* \end{pmatrix} \text{ or } \mathbf{M} \equiv \begin{pmatrix} \cos \mu e^{i\zeta} & \sin \mu e^{-i\vartheta} \\ -\sin \mu e^{i\vartheta} & \cos \mu e^{-i\zeta} \end{pmatrix} (8a)$$

or

$$\mathbf{M} \equiv \frac{1}{\sqrt{1 + |\mathbf{F}|^2}} \begin{pmatrix} e^{-i\Omega} & \mathbf{F}e^{i\Omega} \\ -\mathbf{F} * e^{-i\Omega} & e^{i\Omega} \end{pmatrix}, \tag{8b}$$

where in the second expression μ , ζ , and ϑ are simply real parameters that enforce the required symmetries between the matrix elements. Complex parameter $\mathbb F$ in the last expression represents the output depolarization for a pure (0,1) input; real $\mathbb F$ implies rotational depolarization and imaginary $\mathbb F$ elliptical depolarization. The depolarization is defined as $(E_x/E_z)_{\text{output}}$ when $\vec E_{\text{input}}=\hat z$. [The phase factor Ω is canceled in calculating the depolarization.] Note that the polarization matrices of Equation (8) neglect common attenuation factors and common phase factors.

In our convention, the matrix for the light-valve bottomsurface mirror is $-i\sigma_z$ [since we ignore common phase factors, -i is introduced to preserve the symmetry of Equation (8)], and, neglecting common phase factors, we can use Equations (6) and (7) to obtain the matrix for the dark-state TNLC light valve in reflection:

$$\mathbf{M}_{\mathrm{LV}} \equiv -i\mathbf{M}_{\mathrm{LC}}^{(\mathrm{rev})} \sigma_{z} \mathbf{M}_{\mathrm{LC}}$$

$$= \begin{pmatrix} -i \left[1 - \frac{2\beta^2 \sin^2 \gamma}{\gamma^2} \right] & \frac{2\alpha\beta \sin^2 \gamma}{\gamma^2} \\ + \beta \left(\sin 2\gamma/\gamma \right) & \\ - \frac{2\alpha\beta \sin^2 \gamma}{\gamma^2} & i \left[1 - \frac{2\beta^2 \sin^2 \gamma}{\gamma^2} \right] \\ + \beta \left(\sin 2\gamma/\gamma \right) & \end{pmatrix}$$
(9)

which is equivalent to the result of Lu and Saleh [14], except for sign corrections and conventions.

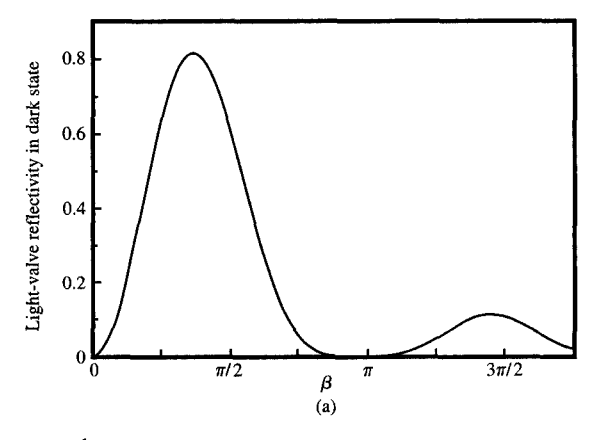
Projection optics that are designed to avoid deliberate depolarization of the beam will tilt surfaces only about rotation axes that are aligned either with, or perpendicular to, the illumination polarization of the central ray. Otherwise, any surface that is tilted by more than ~20° (depending on the coating) is likely to produce a strong "zero-order" depolarization even in the central (i.e., principal) ray of the beam, because of differences in the phase or amplitude of S and P reflectance or transmittance. Even when surface tilts are restricted to the S or P axes of the central ray, compound-angle effects can cause first-order depolarization in off-center rays; this depolarization scales linearly with the difference in skew propagation angle between the off-center ray and the principal ray (linear in amplitude, quadratic in intensity).

For the central ray, however, the curves of Figures 1 and 2 suggest that the PBS-based optical system (with supplemental sheet polarizer) is almost equivalent to ideal crossed polarizers. The light valve then contributes a residual dark-state intensity equal to the square of the off-diagonal elements in Equation (9). In practice, the TN light valve should have non-negligible LC birefringence, so parameter β is unlikely to be small. The off-diagonal elements are zero at $\gamma = \pi$, i.e., at $\beta = \sqrt{\pi^2 - \alpha^2}$. (For simplicity, the case in which γ equals a larger multiple of π is not considered here.) One consideration in choosing the twist angle α is that a high polarization conversion efficiency be obtained when the light valve is driven to maximum brightness; $\alpha = 45^{\circ}$ is a possible choice [23]. Usually $\beta = \pi(n_2 - n_2)d/\lambda$ will only reduce to $\sqrt{m^2\pi^2 - \alpha^2}$

at a single wavelength within the spectral band illuminating the light valve (i.e., where m=1). The light valve background scales with approximately the fourth power of small wavelength shifts away from the center wavelength, as illustrated in **Figure 6**. It should be noted that liquid crystal materials are often highly dispersive in birefringence; $\Delta n \equiv n_c - n_o$ might change by -0.5% for every 1% increase in λ . A more detailed treatment of TNLC reflective light values is given by Yang and Lu [24].

Optical system

The compound-angle properties of a PBS are generic in the sense that the desired S, P performance of such a coating is in itself sufficient to approximately determine the depolarization the coating imposes on skew rays; to wit, the PBS rotates skew-ray polarization by an angle equal to the rotation between the incident and return planes of incidence (as shown in Figure 3). Colorseparating coatings like that in Figure 4 also have a simple performance target, namely that within a particular color band either their reflectance or their transmittance should approach unity. This efficiency goal is usually satisfied fairly well by practical coatings, meaning that at most wavelengths within the color band the coatings will not be amplitude polarizers. Tilted dichroic coatings will be strong amplitude polarizers at the edges of the band, which means that they will tend to be strong phase polarizers throughout the band. (Compactness considerations generally require that the beam be folded at fairly steep angles of incidence.) From an efficiency point of view one would require that the S and P reflectance (or transmittance) be close to unity over most of the band, and that the split between the S and P band edges be as narrow as possible. This represents a qualitative description of the coating's intensity response, and in principle coating phase shifts can be significantly determined by a complete description of the intensity response at all wavelengths [25]. However, in practice the knowledge that available coatings are likely to show high efficiency over most of the band is not sufficient to draw conclusions about phase properties of the coatings. For one thing, designs for tilted color splitters that show low intensity polarization generally achieve this at only one edge of the band [26], whereas the dispersion integrals that link coating intensity and coating phase shift extend over the full spectrum, with a kernel that changes fairly slowly. Second, these dispersion integrals involve the logarithm of the intensity response; a tilted coating would usually be regarded as adequately nonpolarizing in intensity if, for example, the theoretical S transmittance were 10^{-4} and the theoretical P transmittance 10^{-2} , but in such cases the log transmittances still differ appreciably, giving rise to significant S-P relative phase shifts. (The usual "nonpolarizing" edge filter is in fact still polarizing



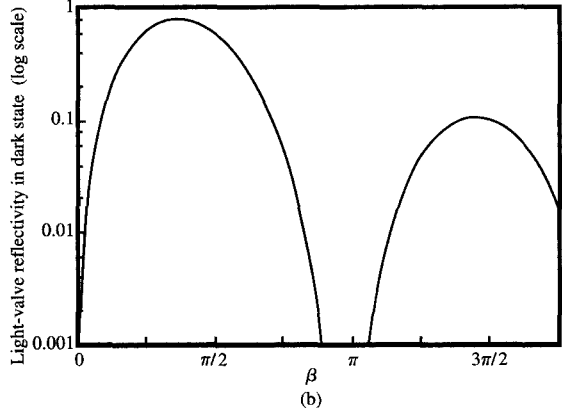


Figure 6

Reflectivity between crossed polarizers of reflective TNLC light valve in dark state (0 voltage) when $\alpha=45^\circ$: (a) Linear scale; (b) log scale. Dark-state reflectivity is zero at $\beta=0.968\pi$. Curves apply when optics NA is negligible.

at the band edge when evaluated on a dB scale.) The S-P phase shifts cause depolarization through the optical system, but, in contrast to the case with the PBS, their effect cannot be calculated or even well estimated without detailed coating prescriptions. The phase shift from dichroic coatings is often appreciable, however. In the center of the reflection band, the first few layers of the coating are sufficient to almost extinguish the transmitted beam, while wavelengths near the band edge penetrate almost to the exit medium. Color-splitting coatings tend to be fairly thick, and for angles of incidence $\approx 20^{\circ}$ there is generally some difference in effective penetration depth between the S and P components, making the coating a phase polarizer.

Specific coating calculations are outside the scope of the present paper. However, we show in this paper that in a

first-order calculation we can define a specific depolarization contribution that is introduced by an individual coated surface; we can then propagate the depolarization as a single quantity from surface to surface. This formulation proves convenient for analyzing the interaction of the optics with the light valve. In the present section of this paper we apply the most common sign convention in thin-film design (see for example Figures 2.1 and 2.2 of Thelen [26]), in which amplitudereflection coefficients are positive when the projections onto the reflecting interface of $\vec{E}_{ ext{Incident}}$ and $\vec{E}_{ ext{reflected}}$ are parallel and negative when antiparallel. (The same convention is used for the transmission coefficients.) We use (0) as a superscript to denote quantities referring to the principal ray (i.e., the central ray of the beam). If $\hat{w}^{(0)}$ represents the direction of the central ray incident on the ith surface, and $\hat{s}^{(0)}$ is a unit vector that defines the direction of S polarization, it is customary in thin-film calculations to choose the sign of $\hat{s}^{(0)}$ according to $\hat{s}^{(0)}_{i+1} \equiv \hat{s}^{(0)}_i \equiv (\hat{w}^{(0)}_i \times \hat{w}^{(0)}_{i+1})/|\hat{w}^{(0)}_i \times \hat{w}^{(0)}_{i+1}|$, where $\hat{w}^{(0)}_{i+1}$ is the reflected ray; thus, the same $\hat{s}^{(0)}$ is used for the incident, reflected, and transmitted rays. The E-field direction in P polarization is then most commonly set to $\hat{p}_i^{(0)} \equiv \hat{s}_i^{(0)} \times \hat{w}_i^{(0)}$ for the incident ray, for the reflected ray to $\hat{p}_{i+1}^{(0)} = \hat{s}_{i+1}^{(0)} \times \hat{w}_{i}^{(0)}$ for the including ray, for the renewed ray, for the renewed to $\hat{p}_{i+1}^{(0)} \equiv \hat{s}_{i+1}^{(0)} \times \hat{w}_{i+1}^{(0)}$. In this convention \hat{s} , \hat{w} , and \hat{p} are not preserved as a right-hand triad, but the S and P reflectances converge to the same value at normal incidence.

We have found proper interpretation of signs to be one of the most time-consuming aspects of correctly calculating depolarization through an optical system. Standard thin-film formalisms serve as a convenient standard for defining the change in electric field at a coated surface. Given the amplitude reflectance ρ and transmittance τ of a coated surface, it is straightforward to propagate the *E*-field from one surface to the next. Applying the Fresnel equation for reflection,

$$\begin{split} \vec{E}_{i+1} &= \rho_{\text{S}}(\vec{E}_i \cdot \hat{s}_i) \hat{s}_i + \rho_{\text{p}}(\vec{E}_i \cdot \hat{s}_i \times \hat{w}_i) (\hat{w}_{i+1} \times \hat{s}_i), \\ \hat{s}_i &= \frac{\hat{w}_i \times \hat{q}_i}{|\hat{w}_i \times \hat{q}_i|}, \\ \hat{w}_{i+1} &= \hat{w}_i - 2(\hat{w}_i \cdot \hat{q}_i) \hat{q}_i, \end{split} \tag{10}$$

where \hat{q}_i is the surface normal; and for transmission,

$$\begin{split} \vec{E}_{i+1} &= \tau_{\mathrm{S}}(\vec{E}_i \cdot \hat{s}_i) \hat{s}_i - \tau_{\mathrm{P}} \frac{\hat{w}_i \cdot \hat{q}_i}{\hat{w}_{i+1} \cdot \hat{q}_i} (\vec{E}_i \cdot \hat{s}_i \times \hat{w}_i) (\hat{w}_{i+1} \times \hat{s}_i), \\ \hat{s}_i &= \frac{\hat{w}_i \times \hat{q}_i}{|\hat{w}_i \times \hat{q}_i|}, \\ \hat{w}_{i+1} &= (\hat{w}_i \cdot \hat{q}_i) \hat{q}_i \sqrt{\frac{(1 - (n_i^2/n_{i+1}^2)}{(\hat{w}_i \cdot \hat{q}_i)^2} + \frac{n_i^2}{n_{i+1}^2} - \frac{n_i}{n_{i+1}}} (\hat{w}_i \times \hat{q}_i) \times \hat{q}_i, \end{split}$$

where n_i and n_{i+1} are the refractive indices. As is usual in thin-film calculations, τ in Equation (11) refers to the tangential components of the *E*-field. The square root in Equation (11) is always taken to be positive. Equations (10) and (11) are expressed in a form that is independent of whether \hat{q}_i is chosen to point "in" to or "out" from the surface (making numerical ray-trace calculations more straightforward), hence the somewhat complicated form chosen for Snell's law in the third line of Equation (11).

Equations (10) and (11) define the electric field throughout the optical system when standard thin-film algorithms are used to calculate the transfer coefficients ρ , τ at the surfaces. The x, y, z components of the E-field are defined in the same global coordinate system as the ray vectors \hat{w}_i and surface normals \hat{q}_i . The equations thus serve as a convenient basis for developing simpler, closed-form solutions [e.g., Equations (19) and (22) below] that maintain a consistent and easily visualized sign convention throughout the system. These first-order solutions can also be derived in a heuristic way, as outlined in the caption of **Figure 7**.

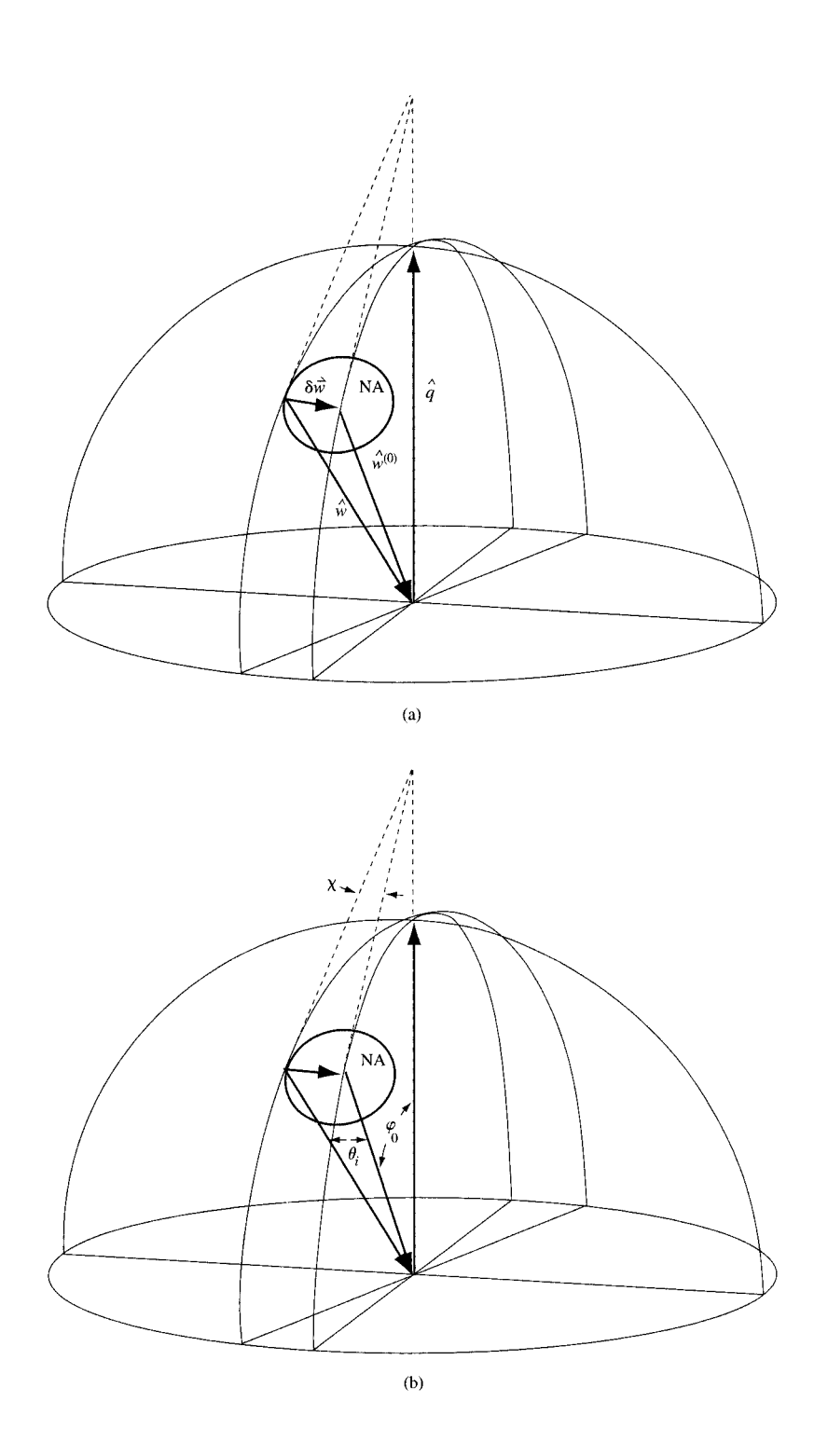
Equations (10) and (11) can also be used in numerical calculations as an alternative to the matrix-based approaches described in the literature (e.g., Waluschka [11]). We pursue them here in order to derive a closed-form first-order equation that propagates the beam depolarization from surface to surface. We have found this first-order analysis to be quite accurate for NAs of interest ($NA \leq 0.14$); in addition, examination of the depolarization contributed by a surface provides useful insight into the nature of the compound-angle contrast loss. The depolarization contributed by a surface to a ray is for our purposes the quantity of direct interest.

A surface-specific beam depolarization should probably only be considered a well-defined quantity in a first-order analysis, because it is only to first order that one can speak of a generic linear polarized beam of finite NA that can serve as a reference. One might arbitrarily choose, for example, a linear dipole pattern as a reference for the general case, but this is a somewhat arbitrary choice, and it would give rise to higher-order terms in the calculated depolarization that would be specific to that choice. However, when the surface is tilted, a unique first-order contribution can be identified.

Consider, for example, reflection of a nominally S-polarized beam whose central ray is pure S-polarized. Figures 7(a) and 7(b) show the reflecting surface as horizontal, with surface normal \hat{q} pointing upward. We can always find quantities E_0 , $\delta E_{i,L}$, and $\delta E_{i,P}$ ($\delta E_{i,L}$ and $\delta E_{i,P}$ are small) that will express the E-field of a particular ray in the beam according to

$$\vec{E}_i = E_0 \hat{s}_i + \delta E_{i,L} \hat{w}_i + \delta E_{i,P} (\hat{w}_i \times \hat{s}_i), \tag{12}$$

because \hat{s}_i , \hat{w}_i , and $(\hat{w}_i \times \hat{s}_i)$ form an orthonormal set. Of



Flaura

Geometry of compound-angle depolarization at coated surface: (a) vectors; (b) angles. The surface normal is \hat{q} . Skew ray \hat{w} is offset by $\delta\vec{w}$ from principal ray $\hat{w}^{(0)}$. Incremental depolarization is approximately proportional to χ , the angle between the planes of P polarization for the two rays. Incremental depolarization is also proportional to (ρ_p/ρ_S-1) or (τ_p/τ_S-1) (for a beam with nominal S polarization), and is therefore zero for a nonpolarizing surface.

course $\delta E_{i,L}$ must equal zero in order that Equation (12) preserve the transversality of the *E*-field (so that $\tilde{E}_i \cdot \hat{w}_i = 0$); however, $\delta E_{i,L}$ becomes nonzero in a first-order expansion (see below). Also, to first order the magnitude squared of Equation (12) is E_0^2 , so that $E_0 \cong E_i$. (In assuming that the depolarization is small compared to that of the overall *E*-field, we are assuming for the time being that ρ_S is large enough that the beam remains predominantly S-polarized after reflection from the surface.) When the skew angle is small, we then have

$$\vec{E}_{i} \cong E_{i}[\hat{s}_{i}^{(0)} - (\delta \vec{w}_{i} \cdot \hat{s}_{i}^{(0)}) \hat{w}_{i}^{(0)}] + \delta E_{i,p}(\hat{w}_{i}^{(0)} \times \hat{s}_{i}^{(0)}), \tag{13}$$

where, as noted above, a superscript (0) is used to denote quantities referring to the central ray (usually these are "zeroth-order" quantities), so that

$$\delta \vec{w}_i \equiv \hat{w}_i - \hat{w}_i^{(0)} \tag{14}$$

represents the propagation angle of the ray within the NA [see Figure 7(a)]. In deriving Equation (13) from Equation (12) we have set $\delta E_{i,L}$ equal to $E_0(\delta \vec{w}_i \cdot \hat{s}_i^{(0)})$, in order that $\vec{E}_i \cdot \hat{w}_i \equiv \vec{E}_i \cdot (\hat{w}_i^{(0)} + \delta \vec{w}_i) = 0$ to first order.

Expanding the second equation in Equation (10), we find, after some algebra,

$$\hat{s}_{i} \cong \hat{s}_{i}^{(0)} - (\hat{s}_{i}^{(0)} \cdot \delta \vec{w}_{i}) \left[\hat{w}_{i+1}^{(0)} - \frac{\hat{q}_{i} \cdot \hat{w}_{i}^{(0)}}{|\hat{q}_{i} \times \hat{w}_{i}^{(0)}|} (\hat{w}_{i+1}^{(0)} \times \hat{s}_{i}^{(0)}) \right], \tag{15}$$

where we have deliberately mixed quantities involving \hat{w}_i and \hat{w}_{i+1} . Similarly,

$$\hat{s}_{i+1}^{(0)} \cdot \delta \vec{w}_{i+1} \cong \hat{s}_{i}^{(0)} \cdot \delta \vec{w}_{i},$$
$$\vec{E}_{i} \cdot \hat{s}_{i} \cong E_{i},$$

$$\vec{E}_i \cdot \hat{s}_i \times \hat{w}_i \cong - \left[\delta E_{i,P} + E_i \frac{\hat{q}_i \cdot \hat{w}_i^{(0)}}{|\hat{q}_i \times \hat{w}_i^{(0)}|} (\hat{s}_i^{(0)} \cdot \delta \vec{w}_i) \right]. \tag{16}$$

If \vec{E}_{i+1} is expressed in the form taken by \vec{E}_i in Equation (13), and then substituted with Equations (13), (15), and (16) into the first line of Equation (10), we obtain in first order

$$\frac{\delta E_{i+1,P}}{E_{i+1}} = -\frac{\rho_{P}}{\rho_{S}} \frac{\delta E_{i,P}}{E_{i}} + \left(\frac{\rho_{P}}{\rho_{S}} - 1\right) \frac{\hat{q}_{i} \cdot \hat{w}_{i}^{(0)}}{|\hat{q}_{i} \times \hat{w}_{i}^{(0)}|} (\hat{s}_{i}^{(0)} \cdot \delta \vec{w}_{i}). \tag{17}$$

The left side of Equation (17) is the cumulative depolarization introduced in the nominally S-polarized beam by the *i*th reflection (and by previous tilted coatings). The factor $\rho_{\rm p}/\rho_{\rm s}$ will be a phase factor if the *i*th surface is lossless (or has equal intensity loss in the two polarizations); this would be the case for a dichroic coating away from the band edge. The $\rho_{\rm p}/\rho_{\rm s}$ factor multiplies any depolarization that may be present in the ray from previous surfaces. The last term on the right can be thought of as the incremental depolarization contributed by skew angle incidence at the *i*th surface. If the angle of incidence of the central ray is $\varphi_{\rm p}$, then the

skew angle $\theta_i \equiv \hat{s}_i^{(0)} \cdot \delta \vec{w}_i$ of the ray is the component of the ray tilt that lies in the direction perpendicular to φ_0 [see Figure 7(b)]. Within the skew meridian, the angle of incidence remains unchanged to first order. Note that while Figure 7 shows $\delta \vec{w}_i$ for the case of a pure skew ray, $\hat{s}_i^{(0)} \cdot \delta \vec{w}_i = \theta_i$ in Equation (17) can represent the skew component of any ray; also, a purely meridional ray at one tilted surface may be a pure skew ray at another surface.

The last term in Equation (17) shows that a tilted surface introduces a depolarization that is linear (in amplitude) with skew angle θ_i . This term contains a factor

$$\chi_i \equiv \frac{\hat{q}_i \cdot \hat{w}_i^{(0)}}{|\hat{q}_i \times \hat{w}_i^{(0)}|} \left(\hat{s}_i^{(0)} \cdot \delta \vec{w}_i \right) = \frac{\theta_i}{\tan \varphi_0}, \tag{18}$$

which is the angle of rotation between the directions of pure P polarization for the ray and for the central ray [see Figure 7(b)]. The remaining factor in the depolarization term, $(\rho_P/\rho_S)-1$, implies that even when the E-field has projections in both the S and P planes, first-order compound-angle depolarization will not take place unless the coating is actually polarizing. This coating factor has a maximum magnitude of 2 (for a coating with 180° S/P phase shift); this is twice as large in amplitude (four times larger in intensity) as the value from a PBS intensity polarizer.

The $(\tan \varphi_0)^{-1}$ dependence of χ in Equation (18) leads to the surprising result that shallow angles of incidence can produce more severe depolarization than steep incidence. Of course, as $\varphi_0 \to 0$ (where our expansion breaks down), a surface becomes nonpolarizing, but for angles of incidence as small as, e.g., 30° (depending on n_i), the S-P phase shift from a dichroic coating can take on essentially any value between 0 and 2π . Since intensity depolarization scales as amplitude squared, a 30° tilted surface can introduce appreciably more depolarization than, say, a 45° surface.

Equation (17) is readily generalized. For example, if many tilted surfaces are traversed, all in a two-dimensional layout, and we consider the tilt of the *i*th surface to arise from rotation of the surface about an axis parallel to $\hat{s}_i^{(0)}$, then because the layout is two-dimensional, these tilt axes will all be parallel to the tilt axis $\hat{s}_{PBS}^{(0)}$ of the PBS. In this case we find that for each surface,

$$\frac{\delta E_{i+1}}{E_{i+1}} = \xi_i \left[\eta_i \frac{\delta E_i}{E_i} - \kappa_i (\eta_i - 1) \frac{\theta_0}{n_i \tan \varphi_{0,i}} \right], \tag{19}$$

where $\xi_i = +1$ if the ray follows the transmitted path through the surface, and -1 if it follows the reflected path. η_i is defined as $(\rho_{\rm p}/\rho_{\rm S})$ for a reflected ray and as $(\tau_{\rm p}/\tau_{\rm S})$ for a transmitted ray. n_i is the refractive index in the incident space at the *i*th surface, and θ_0 is the skew angle of the ray as measured in air. θ_0 is invariant through the system. The beam angle of incidence $\varphi_{0,i}$ is always taken as positive. The sign of the surface depolarization

is governed by parameter κ , which essentially specifies whether the surface tilt is oriented so as to deviate the reflected ray clockwise or counterclockwise; κ is defined as

$$\kappa_{i} \equiv \begin{cases}
+1 & \text{if } \hat{w}_{i}^{(0)} \times \hat{w}_{i+1}^{(0)} \cdot \hat{s}_{PBS}^{(0)} > 0, \\
-1 & \text{if } \hat{w}_{i}^{(0)} \times \hat{w}_{i+1}^{(0)} \cdot \hat{s}_{PBS}^{(0)} < 0.
\end{cases}$$
(20)

[Note that the $\hat{w}_{i+1}^{(0)}$ appearing in Equation (20) always refers to the reflected ray, even when the depolarization is being calculated for the transmitted beam.]

In the general case where the layout is not twodimensional, i.e., at least one surface i is tilted about the axis perpendicular to the tilt axis of the PBS hypotenuse, Equation (19) still applies if 1) the angle θ_0 is replaced by ψ_0 , again defined as $\hat{s}_i^{(0)} \cdot \delta \vec{w}_i$ (which for an orthogonally tilted surface will be in the meridian perpendicular to θ_0), 2) parameter η_i is defined as $\rho_{\rm S}/\rho_{\rm P}$ or $\tau_{\rm S}/\tau_{\rm P}$, and 3) the definition of κ_i in Equation (20) is multiplied by -1.

Equation (19) can be rewritten in a number of ways; for example, we can propagate the depolarization in the ray relative to the tilted ray-specific P direction according to

$$\begin{split} \left(\frac{\delta E}{E} - \frac{\theta_0 \kappa}{n \tan \varphi_0}\right)_{i+1} &= \xi_i \eta_i \left(\frac{\delta E}{E} - \frac{\theta_0 \kappa}{n \tan \varphi_0}\right)_i \\ &- \theta_0 \left[\frac{\kappa_{i+1}}{n_{i+1} \tan \varphi_{0,i+1}} - \frac{\kappa_i \xi_i}{n_i \tan \varphi_{0,i}}\right]. \end{split}$$

If the *i*th and i+1th surfaces are parallel and in the same medium, the term in square brackets is zero (because $\kappa_{i+1} = \kappa_i \xi_i$ when the surfaces are parallel); in such a case Equation (21) shows that the surface contributes no relative depolarization.

As a linear difference equation, Equation (19) is easy to solve for an arbitrary succession of $j=0,\cdots,J$ tilted interfaces (starting from j=0 at the PBS). The closed-form solution is

$$\frac{\delta E_{J+1}}{E_{J+1}} = -\left(\prod_{j=1}^{J} \xi_{j} \eta_{j}\right) \kappa_{0} \frac{\theta_{0}}{n_{\text{PBS}}} - \sum_{j=1}^{J} \left[\xi_{j} \kappa_{j} (\eta_{j} - 1) \left(\prod_{k=j+1}^{J} \xi_{k} \eta_{k}\right) \frac{\theta_{0}}{n_{j} \tan \varphi_{0, j}}\right]. \tag{22}$$

We should note that Equations (19) and (22) have one limitation that is not easily generalized out. If the beam path includes tilted interfaces at which the rays are transmitted, these interfaces must arise in pairs analogous to the front and back surface of a tilted parallel plate; i.e., a tilted transmission interface must be followed by a parallel transmission interface, and the exit refractive index must equal the incident index at the first interface. The intervening space can then be treated as a thick incoherent layer. Thus, the first-order formalism applies to

a tilted air space, or to front-side and back-side coatings on a tilted dichroic mirror, but not to a refractive prism. Elements with wedge give rise to strong aberrations and so would not ordinarily be used in a projection display; Equations (10) and (11) are available for numerical solution in such a case. [Equations (19) and (22) have no restriction on traversal of interfaces at angles near normal incidence, i.e., interfaces that are only slightly tilted.]

Contrast loss from interaction between light valve and optical system

The methods of the previous section can be used to propagate the E-field to and from the light valve. An earlier section presented analysis to account for the polarization properties of the light valve itself. Together these constitute a solution for the contrast loss through the optical system. However, with one further restriction we can establish solutions that are easily written in a simpler and more compact form, but which still represent fairly general descriptions of the interaction. So long as the only lossy element in the path is the PBS (the PBS is lossy in the sense that it directs some light into a different path), we show that we can describe the interaction with the light valve purely in terms of the rotation and ellipticity that the optics induce on the illumination. Under this restriction we treat coatings in the system other than the PBS as phase polarizers; $\rho_{\rm p} = e^{i\Delta_{\rm p}}$ and $\rho_{\rm s}=e^{i\Delta_{\rm S}}$. As noted above, the optical coatings in a given color channel are designed to be as efficient as possible, and losses are usually small except at the edges of the band. We have found in numerical calculations that phase effects often dominate over amplitude effects even near the band edges, and the accuracy of the phase-only approximation becomes quite good when dark-state intensity contributions are integrated over the entire color band.

The assumption of lossless elements (or, more precisely, the assumption that elements have equal loss in S and P polarization) is not necessary in using the equations of the previous sections. The advantage of such an assumption is that it allows us to employ the symmetries in Equations (7) and (8). Unfortunately, while Equation (19) is based on the most common sign convention in thin-film design (see, for example, Thelen [26]), the most common Jonesmatrix sign convention [22] is incompatible because it preserves as a right-handed triad the two polarization basis directions and the ray direction. To express Equation (19) in the matrix sign convention, we briefly adopt a somewhat awkward notation in order to introduce absolute phase factors that maintain the symmetry of Equation (8) independent of whether ξ equals +1 or -1. Specifically, we write i in the form $i = \sqrt{\xi}$ for the case $\xi = -1$; when $\xi = +1$, this $\sqrt{\xi}$ factor is unity. The Jones-matrix form of Equation (19) can then be written:

$$2\frac{\kappa_{i}}{\sqrt{-\xi_{i}}}\sin\left(\frac{\Delta_{p}-\Delta_{S}}{2}\right)\frac{\theta_{0}}{n_{i}\tan\varphi_{0,i}}\left(\frac{\delta E_{i}}{E_{i}}\right).$$

$$\frac{e^{-i(\Delta_{p}-\Delta_{S})/2}}{\sqrt{\xi_{i}}}$$
(23)

Note that Equation (23) is in a form in which an additional matrix for rotation of the S, P axes to propagate to the next surface is unnecessary. Equation (23) is most naturally associated with a different sign convention from that of Equation (19); the difference is essentially that in Equation (23) the projections onto the surface of the reflected and incident unit vectors \hat{p}_{refl} , \hat{p}_{inc} for P polarization are antiparallel. The $\sqrt{\xi}$ factor outside the matrix is included in Equation (23) for consistency with Equation (19); however, since its value is either ior 1, it represents a common phase factor and can be dropped; $e^{i(\Delta_P + \Delta_S)/2}$ is likewise a common phase factor. In this part of the paper we assume equal efficiency in S and P polarizations; any common attenuation factor is also dropped if system contrast is the quantity of interest.

The diagonal elements of the matrix of Equation (23) have magnitude unity; the off-diagonal elements are firstorder quantities proportional to the skew angle θ_0 . When two such matrices are multiplied together, the product matrix preserves this structure to first order. An equivalent statement is that the multisurface solution in Equation (22) exhibits this form when written as a matrix.

Since the optical system should not depolarize the central ray, we can assume that all surfaces are tilted about axes that are either parallel to the $\hat{s}_{PBS}^{(0)}$ tilt axis of the PBS hypotenuse, or are perpendicular to it. A ray can be parametrized by the skew angle θ_0 it makes to the PBS hypotenuse (scaled for air, n = 1), and by an orthogonal angle ψ_0 . θ_0 and ψ_0 thus represent an orthogonal pair of pupil coordinates which range between -NA and +NA(with $\sqrt{\theta_0^2 + \psi_0^2} \le NA$). Excluding the PBS, the Jones matrix for the optical system then takes the form

$$\mathbf{M}_{\text{Non-PBS optics}} = \begin{pmatrix} e^{i\Sigma/2} & \nu_{\theta}\theta_{0} + \nu_{\psi}\psi_{0} \\ -\nu_{\theta}^{*}\theta_{0} - \nu_{\psi}^{*}\psi_{0} & e^{-i\Sigma/2} \end{pmatrix}, \tag{24}$$

where ν_a , ν_a , and Σ are determined by the methods of the previous section. In first order the illumination matrix for the PBS is

$$\mathbf{M}_{\text{PBS}} = \begin{pmatrix} 0 & -\theta_0' \\ \theta_0' & 1 \end{pmatrix}, \tag{25}$$

where $\theta_0' \equiv \theta_0/n_{\rm PBS}$ is the skew angle of incidence inside the PBS. (For the time being we assume a 45° cube PBS.) Assuming as an input, for example, unpolarized light, the Jones vector for the E-field illuminating the light valve

will then take the form

$$\begin{pmatrix} \delta E \\ E \end{pmatrix} \cong \begin{pmatrix} -\theta_0 e^{i\Sigma/2} / n_{\text{PBS}} + \nu_\theta \theta_0 + \nu_\psi \psi_0 \\ e^{-i\Sigma/2} \end{pmatrix}, \tag{26}$$

where second-order terms are dropped. The depolarization of the illumination then takes the form

$$\frac{\delta E}{E} = -\theta_0 [e^{i\Sigma}/n_{PBS} - \nu_\theta e^{i\Sigma/2}] + \psi_0 [\nu_\psi e^{i\Sigma/2}]. \tag{27}$$

For small depolarization, the real part of $\delta E/E$ represents a rotation in the illuminating polarization and the imaginary part an ellipticity. According to Equation (27), a ray in the skew meridian to the PBS ($\psi_0 = 0$) will have rotation and ellipticity that are proportional to θ_0 , while for a ray in the orthogonal meridian, rotation and ellipticity will be proportional (with different constants of proportionality) to ψ_0 . Let us denote these constants of proportionality as $\mathfrak{R}_{_{\theta}},\,\mathfrak{I}_{_{\theta}},\,\mathfrak{R}_{_{\psi}},\,\mathfrak{R}_{_{\psi}},\,\mathfrak{R}$ represents rotation in the sense that the optical coatings introduce R radians of polarization rotation per radian of skew angle in a ray illuminating the light valve; similarly, the induced ellipticity is 3 in the sense that the aspect ratio of a rectangle which circumscribes the polarization ellipse will be $\Im \theta$ when the ray skew angle is θ (θ assumed small). Note that while rotation and ellipticity are considered small (proportional to θ , ψ), the constants of proportionality \Re , \Im may have appreciable magnitude.

We now can write Equation (24) as

$$\mathbf{M}_{\text{Non-PBS optics}} = \begin{pmatrix} 1 & \mathcal{P}_{\boldsymbol{\theta}} \boldsymbol{\theta}_0 + \mathcal{P}_{\boldsymbol{\psi}} \boldsymbol{\psi}_0 \\ -\mathcal{P}_{\boldsymbol{\theta}}^* \boldsymbol{\theta}_0 - \mathcal{P}_{\boldsymbol{\psi}}^* \boldsymbol{\psi}_0 & 1 \end{pmatrix} \mathbf{M}_{\text{OptPhase}}, \tag{28}$$

where

$$\begin{split} \mathcal{P}_{\theta} &\equiv (\mathfrak{R}_{\theta} + i\mathfrak{T}_{\theta}) + e^{i\Sigma}/n_{\text{PBS}} = \nu_{\theta} e^{-i\Sigma/2}, \\ \mathcal{P}_{\psi} &\equiv (\mathfrak{R}_{\psi} + i\mathfrak{T}_{\psi}) = \nu_{\psi} e^{-i\Sigma/2}, \end{split} \tag{29}$$

$$\mathbf{M}_{\text{OptPhase}} = \begin{pmatrix} e^{i\Sigma/2} & 0\\ 0 & e^{-i\Sigma/2} \end{pmatrix}. \tag{30}$$

Equation (29) obtains because, when substituted [together with Equation (30)] into Equation (28) and compared with Equation (24), the expressions obtained for ν_{θ} , ν_{tt} give the

correct result when substituted into Equation (27), namely $\delta E/E = (\mathfrak{R}_{\theta} + i\mathfrak{F}_{\theta})\theta_{0} + (\mathfrak{R}_{\psi} + i\mathfrak{F}_{\psi})\psi_{0}$; we have defined the parameters \mathfrak{R}_{θ} , \mathfrak{F}_{θ} , \mathfrak{R}_{ψ} , \mathfrak{F}_{ψ} by the requirement that the depolarization $\delta E/E$ take this form. In other words, Equations (28)–(30) represent the optical system in terms of the rotation \mathfrak{R} and ellipticity \mathfrak{F} it imposes on skew rays incident at the light valve.

We now represent M_{PBS} [Equation (25)] as

$$\mathbf{M}_{\mathrm{PBS}} = \begin{pmatrix} 0 & -\theta_0/n_{\mathrm{PBS}} \\ \theta_0/n_{\mathrm{PBS}} & 1 \end{pmatrix} \Rightarrow \mathbf{M}_{\mathrm{Rot}} \mathbf{M}_{\mathrm{PrePol}}, \tag{31}$$

where

$$\mathbf{M}_{\mathrm{Rot}} \equiv \begin{pmatrix} 1 & -\theta_0/n_{\mathrm{PBS}} \\ \theta_0/n_{\mathrm{DBS}} & 1 \end{pmatrix}$$

and

$$\mathbf{M}_{\mathsf{PrePol}} \equiv \begin{pmatrix} 0 & 0 \\ 0 & 1 \end{pmatrix}. \tag{32}$$

Note that M_{PrePol} is taken to represent part of the PBS operation. The projector might also include a sheet polarizer (at least in the reflection pass) to ensure adequate rejection, but with or without such a supplementary polarizer the system must perform an operation equivalent to M_{PrePol} .

Using Equation (31), we can now write the first-order matrix for the optics (illuminating in single pass) as

$$M_{\text{Optics}} = M_{\text{Non-PBS optics}} M_{\text{PBS}}$$

$$\equiv M_{\text{OpticsAll}} M_{\text{PrcPol}}, \qquad (33)$$

where $M_{OpticsAll}$ combines the M_{Rot} rotation from the PBS [Equation (32)] with the non-PBS optical elements [$M_{Non-PBS\ optics}$ given in Equations (24) and (28)], and can be written as

$$M_{\text{OpticsAll}} \equiv M_{\text{Perturb}} M_{\text{OptPhase}}, \qquad (34)$$

where

$$\mathbf{M}_{\mathrm{Perturb}} \equiv \begin{pmatrix} 1 & \left[\mathfrak{R}_{\boldsymbol{\theta}} + i \mathfrak{I}_{\boldsymbol{\theta}} \right] \boldsymbol{\theta}_0 \\ & + \left[\mathfrak{R}_{\boldsymbol{\psi}} + i \mathfrak{I}_{\boldsymbol{\psi}} \right] \boldsymbol{\psi}_0 \\ \\ - \left[\mathfrak{R}_{\boldsymbol{\theta}} - i \mathfrak{I}_{\boldsymbol{\theta}} \right] \boldsymbol{\theta}_0 & 1 \\ - \left[\mathfrak{R}_{\boldsymbol{\psi}} - i \mathfrak{I}_{\boldsymbol{\psi}} \right] \boldsymbol{\psi}_0 \end{pmatrix},$$

and where $M_{OptPhase}$ is defined in Equation (30). For compactness we now introduce a vector notation for the pupil coordinates in which we denote the ray-propagation angle as $\hat{\theta} \equiv (\theta_0, \psi_0)$. Defining

$$\vec{P} = \vec{R} + i\vec{I} = ([\mathfrak{R}_{\theta} + i\mathfrak{R}_{\theta}], [\mathfrak{R}_{\theta} + i\mathfrak{R}_{\theta}]), \qquad (36)$$

we have

$$\mathbf{M}_{\text{Perturb}} = \begin{pmatrix} 1 & \vec{P} \cdot \vec{\theta} \\ -\vec{P}^* \cdot \vec{\theta} & 1 \end{pmatrix}. \tag{37}$$

 $\vec{P} \cdot \vec{\theta}$ is the depolarization $\delta E/E$ in the light incident on the light valve. The single (illumination)-pass matrix for the optical system is now

$$\mathbf{M}_{\text{Ontics}} = \mathbf{M}_{\text{Perturb}} \mathbf{M}_{\text{OntPhase}} \mathbf{M}_{\text{PrePol}}.$$
 (38)

To propagate through the system in double pass (illumination and collection), we must determine the matrix for reverse propagation along the sequence of Equation (38). All component matrices in Equation (38) except for M_{PrePol} are assumed to exhibit equi-S-P efficiency. We first note, therefore, that given our sign convention the matrices other than M_{PrePol} are reversible in a strict sense according to the rule of Equation (7) above. For example, if we were to apply Equation (7) directly to Equation (37) we would obtain

$$\mathbf{M}_{\text{Perturb}}^{(\text{rev})} = \begin{pmatrix} 1 & \vec{P}^* \cdot \vec{\theta} \\ -\vec{P} \cdot \vec{\theta} & 1 \end{pmatrix}. \tag{39}$$

However, Equation (7) applies to a true "time reversal," in which the rays are made to exactly retrace their incoming paths. In a projector, the rays that reflect from the light valve return to the optical system through the opposite side of the lens pupil. As noted in the introduction, this means that the optics obey a reversal symmetry opposite to that of the light-valve active layer. If we denote the reversal that applies to the optics using a superscript (MirRev), we have, in analogy with Equation (7),

$$\mathbf{M}^{\text{(MirRev)}}[\vec{\theta}] = \begin{pmatrix} m_{11}[-\vec{\theta}] & -m_{21}[-\vec{\theta}] \\ -m_{12}[-\vec{\theta}] & m_{22}[-\vec{\theta}] \end{pmatrix}, \tag{40a}$$

when

$$M[\vec{\theta}] = \begin{pmatrix} m_{11}[\vec{\theta}] & m_{12}[\vec{\theta}] \\ m_{21}[\vec{\theta}] & m_{22}[\vec{\theta}] \end{pmatrix}. \tag{40b}$$

In Equation (9) we derived the dark-state matrix for a TNLC light valve, but for the moment we consider the general case in which the light valve has matrix elements g_{11} , g_{12} , g_{21} , g_{22} ; we can alternatively define the general light valve by parameters a_1 , a_2 , a_3 , a_4 , where

$$\mathbf{M}_{LV} = \begin{pmatrix} g_{11} & g_{12} \\ g_{21} & g_{22} \end{pmatrix} \equiv a_1 \mathbf{I} + a_2 \sigma_x + a_3 \sigma_y + a_4 \sigma_z. \tag{41}$$

with the σ matrices defined in Equation (4). Using Equations (33) and (34), we have

$$\mathbf{M}_{\text{Projector}} \equiv \begin{pmatrix} 1 & 0 \\ 0 & 0 \end{pmatrix} \begin{pmatrix} e^{i\Sigma/2} & 0 \\ 0 & e^{-i\Sigma/2} \end{pmatrix} \begin{pmatrix} f_{11} & f_{12} \\ f_{21} & f_{22} \end{pmatrix} \begin{pmatrix} e^{i\Sigma/2} & 0 \\ 0 & e^{-i\Sigma/2} \end{pmatrix} \begin{pmatrix} 0 & 0 \\ 0 & 1 \end{pmatrix}, \tag{42a}$$

where
$$\begin{pmatrix} f_{11} & f_{12} \\ f_{21} & f_{22} \end{pmatrix} \equiv \mathbf{M}_{\text{Perturb}}^{\text{(MirRev)}} (a_1 \mathbf{I} + a_2 \sigma_x + a_3 \sigma_y + a_4 \sigma_z) \mathbf{M}_{\text{Perturb}}$$
. (42b)

In obtaining Equation (42) we have made use of the fact that while the M_{Rot} component in $M_{Perturb}$ [see Equations (31)–(34) above] reverses according to Equation (40), on the collection pass the M_{PrePol} factor in M_{PBS} will take the form of the leftmost matrix on the right of Equation (40); in this form the polarizer matrix passes bright-state light to the projection lens.

From Equation (42a) we obtain

$$\mathbf{M}_{\text{Projector}} = \begin{pmatrix} 0 & f_{12} \\ 0 & 0 \end{pmatrix}. \tag{43}$$

The birefringencelike phase term Σ in the optics [from matrix M_{OptPhase} in Equation (30)] thus cancels out in the expression for double-pass propagation through the optics, though it appears implicitly in the elements of M_{Perturb} .

We now define B as the residual dark-state intensity transmitted by the projector. If the efficiencies in the dark state and bright state are equal, B will be the reciprocal of the contrast ratio. We have, from Equations (37) and (40)–(43),

The light-valve matrix M_{LV} in Equation (9) assumes the specific TNLC form [Equation (6)] for the matrix M_{LC} of the active layer above the mirror backplane. If we instead allow a more general form for the dark-state matrix of the active layer, which we denote as M_{Active} in this more general case, requiring only that M_{Active} satisfy the equi-S-P efficient condition of Equation (8), then using $M_{LV} \equiv -i M_{Active}^{(rev)} \sigma_z M_{Active}$ and applying Equation (41), we find

$$a_1 = 2 \sin^2 \mu \sin 2\vartheta + 2 \cos^2 \mu \sin 2\zeta,$$

 $ia_4 = -2 \sin^2 \mu \cos 2\vartheta - 2 \cos^2 \mu \cos 2\zeta,$ (47)

where ζ , ϑ , and μ are the parameters appearing in the second representation given in Equation (8) (as applied to the active layer), obtaining finally

$$B = g_{12}^{2} + 4(\vec{\theta} \cdot \text{Im}[g_{11}\vec{P}])^{2}$$

$$= g_{12}^{2} + 16(\vec{\theta} \cdot [(\sin^{2} \mu \sin 2\vartheta + \cos^{2} \mu \sin 2\zeta)\vec{I} + (\sin^{2} \mu \cos 2\vartheta + \cos^{2} \mu \cos 2\zeta)\vec{R}])^{2}.$$
(48)

$$\mathbf{B} = |f_{12}|^2 = \left| \left\{ \begin{pmatrix} 1 & -\vec{P}^* \cdot \vec{\theta} \\ \vec{P} \cdot \vec{\theta} & 1 \end{pmatrix} \begin{pmatrix} g_{11} & g_{12} \\ g_{21} & g_{22} \end{pmatrix} \begin{pmatrix} 1 & \vec{P} \cdot \vec{\theta} \\ -\vec{P}^* \cdot \vec{\theta} & 1 \end{pmatrix} \right\}_{12} \right|^2, \tag{44}$$

where $\{ \}_{12}$ denotes the 1, 2 matrix element. Substituting from Equations (4), (36), and (41),

$$B = \left| \{ (I + i[\vec{I}\sigma_{r} - \vec{R}\sigma_{v}] \cdot \vec{\theta}) (a_{1}I + a_{2}\sigma_{r} + a_{3}\sigma_{v} + a_{4}\sigma_{z}) (I + i[\vec{I}\sigma_{r} + \vec{R}\sigma_{v}] \cdot \vec{\theta}) \}_{12} \right|^{2}. \tag{45}$$

Note that the vector quantities in Equation (45) refer to the two-dimensional space of pupil coordinates θ_0 , ψ_0 . The x, y, z subscripts on the Pauli matrices are standard notation but do not refer to physical coordinates in our application.

Applying the multiplication rules for the Pauli matrices [20] and keeping only first-order terms in $\vec{\theta}$, we find

$$\mathbf{B} \cong |g_{12} + 2i\vec{\theta} \cdot (a_1\vec{I} - ia_4\vec{R})|^2 = |g_{12} + 2i\vec{\theta} \cdot \operatorname{Im} [g_{11}\vec{P}]|^2.$$
(46)

According to Equation (46), the off-diagonal element g_{12} of the light-valve matrix contributes to system background B via direct depolarization, while the diagonal elements (which determine a_1 and a_4 , and which represent effects such as birefringence) interact with the optics via the rotation and ellipticity parameters \vec{R} and \vec{I} to produce contrast loss.

Equation (48) takes g_{12} to be pure real; this follows from the assumption that $\mathbf{M}_{LV} \equiv -i\mathbf{M}_{Active}^{(rev)}\boldsymbol{\sigma}_z\mathbf{M}_{Active}$, with \mathbf{M}_{Active} satisfying Equation (8).

We can also use the third form of Equation (8) to describe the active-layer matrix; expressed in this form, we find

$$\mathbf{B} = \frac{4}{(1 + \mathbb{F}'^2 + \mathbb{F}''^2)^2} \{ \mathbb{F}''^2 + (\vec{\theta} \cdot [([1 + \mathbb{F}'^2 - \mathbb{F}''^2] \sin 2\Omega)] + [2\mathbb{F}'\mathbb{F}''] \cos 2\Omega) \vec{I} + ([1 + \mathbb{F}'^2 - \mathbb{F}''^2] \cos 2\Omega - [2\mathbb{F}'\mathbb{F}''] \sin 2\Omega) \vec{R}])^2 \}, \quad (49)$$

where \mathbb{F}' and \mathbb{F}'' represent the real and imaginary parts of the depolarization \mathbb{F} of the central ray at the mirror backplane of the light valve. Equation (49) shows that without the optical system (i.e., $\theta \to 0$), contrast loss arises only when the light reaching the mirror backplane has elliptical depolarization (so that the first term \mathbb{F}''^2 in the curly brackets is nonzero); however, when $\theta \neq 0$, the optical system interacts with both rotational and elliptical depolarization in the active layer of the light valve to produce contrast loss in the image. A hypothetical ideal light-valve active layer which (in dark state) produced linear polarization at all depths above the mirror backplane (and at all wavelengths) would satisfy $\mathbb{F}'' = 0$ but would nonetheless show contrast loss in most optical systems of finite NA.

Equations (48) and (49) represent fairly general expressions for the contrast loss along a ray, subject only to the first-order approximation that the total depolarization in the optics is small, and to the approximation that optical elements other than the PBS polarize in phase and not amplitude. Note that Equation (48) involves no complex parameters [and Equation (49) uses real and imaginary parts explicitly]. The g_{12} direct depolarization from the light valve makes a contribution to the intensity that is independent of the second term in Equation (48); i.e., the two terms add incoherently. The second term does, however, represent a coherent interaction between the optics and the diagonal matrix elements of the light valve.

We must average Equation (48) over the full cone of rays in the pupil to obtain the actual dark-state background in the projected image. We first introduce the shorthand notation

$$\vec{F} = [F_{\theta}, F_{\phi}] = 2[(\sin^2 \mu \sin 2\vartheta + \cos^2 \mu \sin 2\zeta)\vec{I} + (\sin^2 \mu \cos 2\vartheta + \cos^2 \mu \cos 2\zeta)\vec{R}]. \quad (50)$$

The pupil radius is NA, and we assume the illumination intensity to be uniform over this circular cone; however, to allow for nontelecentricity and misalignment we average Equation (48) over the two-dimensional θ_0 , ψ_0 domain having boundary

$$\sqrt{(\theta_0 - \theta_{\text{Decenter}})^2 + (\psi_0 - \psi_{\text{Decenter}})^2} \le NA, \tag{51}$$

where $\theta_{\rm Decenter}$ and $\psi_{\rm Decenter}$ are constants representing the nontelecentricity or misalignment at a particular field location.

Carrying out the average over the circular pupil domain of Equation (51), we find

$$\langle B \rangle_{NA} = g_{12}^2 + (F_{\theta}^2 + F_{\psi}^2) N A^2 + 4(F_{\theta} \theta_{Decenter} + F_{\psi} \psi_{Decenter})^2.$$
 (52)

Equation (52) indicates that contrast loss (essentially

 $1/\langle B \rangle$) scales quadratically with the angular extents of the beam. The factor of 4 in the third term indicates that contrast loss is fairly sensitive to nontelecentricity in the optics.

• Particular cases

We now apply our result from Equation (52) in a number of specific cases.

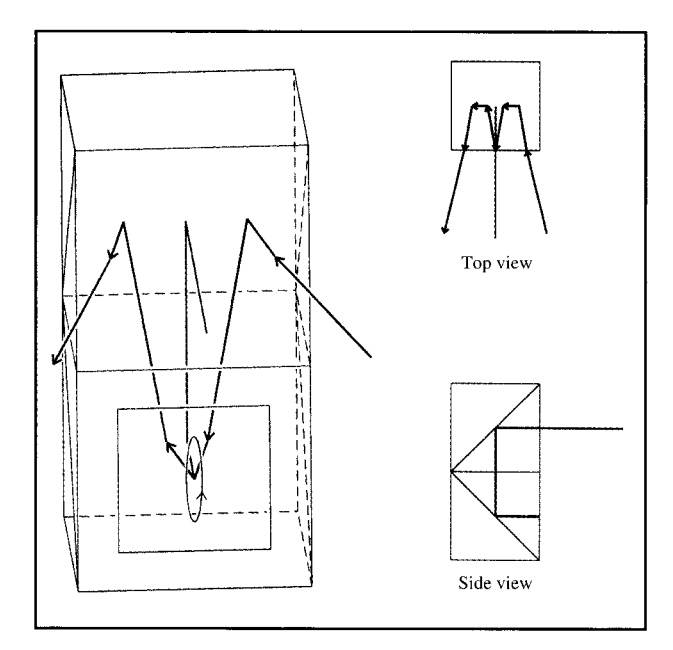
1. Two-dimensional optical layout; polarizing surfaces tilted about common axis

Considering for simplicity the telecentric case, if all polarizing surfaces in the optics (including the PBS) are tilted within a common plane (i.e., rotation axes for all surface tilts are perpendicular to this plane), Equation (52) becomes

$$\begin{split} \langle \mathbf{B} \rangle_{\mathrm{NA}} &= g_{12}^2 + F_{\theta}^2 N A^2 \\ &= g_{12}^2 + 4([\sin^2 \mu \sin 2\vartheta + \cos^2 \mu \sin 2\zeta] \Im_{\theta} \\ &+ [\sin^2 \mu \cos 2\vartheta + \cos^2 \mu \cos 2\zeta] \Re_{\theta})^2 N A^2. \end{split} \tag{53}$$

By definition, the θ meridian is always chosen to include the tilt axis of the PBS hypotenuse [i.e., the $\hat{s}_{PBS}^{(0)}$ axis about which the PBS hypotenuse is effectively rotated in order to be tilted against the beam], so that θ represents the skew angle of the ray against the PBS. In a twodimensional layout where the tilt axes of all surfaces are parallel, the ψ coordinate does not affect depolarization. Conversely, in a non-two-dimensional (but telecentric) system where each meridian serves as the skew meridian for at least one surface, Equation (52) indicates that each meridian will make an independent contribution to the dark-state background (assuming, as we have, a uniform circular pupil). Background will often be less when all surfaces are tilted about a common axis, because the ψ meridian then contributes zero background. However, in the general case the contribution made by each meridian takes the same form, so for brevity we exhibit most of the following results for the case of parallel surface-tilt axes and telecentric optics.

Note that even though the θ and ψ ray components make independent contributions to the intensity background of Equation (52), it should not be concluded that optical surfaces tilted in one meridian have effects independent of those of surfaces tilted in the other. In general, an optical surface which is tilted in one meridian will still make a contribution to the parameters \Im and \Re for the other meridian, except in the particular case where all surfaces are tilted about parallel tilt axes; in this special case we have seen that \Im_{ψ} and \Re_{ψ} vanish, as in Equation (53). In general, Equation (19) shows that once a ray has become depolarized, succeeding surfaces usually



Correction of compound-angle depolarization with mirrorlike light valve. If single-pass depolarization of illuminating skew ray is purely elliptical (as in figure), symmetry causes depolarization to cancel in return pass through optical system. Depolarization that is purely rotational will double. Different symmetries apply when the dark state of the light valve is not mirrorlike [see Equation (57)].

introduce additional changes in polarization even when the ray has no skew incidence component.

2. Light valve has mirrorlike dark state In this case $\mu=0$ and $\zeta=\pi/2$ in Equation (8), and Equation (53) becomes

$$\langle \mathbf{B} \rangle_{NA} = g_{12}^2 + \Re_{\theta}^2 NA^2,$$
 (54)

where for simplicity we have assumed telecentric optics in which the tilt axes for all polarizing coatings are parallel. Parameter 3 does not appear in Equation (54), showing that skew-ray ellipticity introduced by the optics will cancel out in double pass if the light valve is mirrorlike; i.e., elliptical depolarization in the optics will not cause dark-state background. Recall that in our first-order treatment we expand the depolarization against axes corresponding to the central ray, denoted by a superscript (0). [An exception was made to this approach in Equation (21).] The rotation \Re of concern in Equation (54) is thus a rotation relative to the plane of incidence (at tilted coatings) of the central ray, evaluated when the ray illuminates the light valve. This is illustrated in Figure 8, which shows schematically the polarization ellipse of a skew ray illuminating a light valve in an optical system

with two tilted coatings. In the figure the ray reflects from two tilted surfaces which are hypotenuse surfaces in the two cube elements. Once the incident ray reflects from the second hypotenuse coating, it is traveling out of the perspective diagram toward the viewer; it then illuminates a light valve on the front surface of the bottom cube. The figure shows the case in which the optical system introduces ellipticity but not rotation. The major axis of the skew ray's ellipse is therefore aligned with the plane of the central ray. (The central ray is shown in green.) Because of this alignment the folded path of the central ray then forms a plane of symmetry for the electric field as well as for the rays. Equation (54) shows that because of this symmetry the depolarization is canceled out in the return pass through the optics.

On the other hand, rotational depolarization doubles in amplitude in the round trip [i.e., quadruples in intensity; the resulting factor of 4 is canceled in Equation (54) when θ is averaged over the pupil]. Of course, the actual polarization state of the round-trip light is determined by the pass direction of the PBS at the exit face; the implication of Equation (54) is that, when the single-pass depolarization is purely rotational, the dark-state intensity measured in double pass will be four times larger than the intensity measured in single pass between crossed polarizers.

3. Light valve is "ideal"

A dark-state light valve can be considered nominally ideal if its reflectivity between crossed polarizers is zero. An ideal light valve is not necessarily mirrorlike in the dark state; the requirement that its off-diagonal elements be zero means that when the matrix for the active layer of the light valve is expressed in the third form of Equation (8), parameter $\mathbb F$ must be pure real. A light valve that is ideal in this sense will not necessarily have zero dark-state intensity when used in an optical system. Considering for simplicity the case of a telecentric system with a two-dimensional layout, Equations (49) and (52) become

$$\langle B \rangle_{NA} = NA^2 [\Im_{\theta} \sin 2\Omega + \Re_{\theta} \cos 2\Omega]^2.$$
 (55)

An ideal light valve must have a dark state that is essentially equivalent to a retarder placed over a mirror (with the retarder axes aligned with the polarization of the illuminating central ray). If the equivalent retarder for such an ideal light valve is quarter-wave, $2\Omega = 90^{\circ}$, and the dark-state intensity will be zero in an optical system that induces no ellipticity in the illumination. On the other hand, if the light valve is equivalent to a mirror (case 2 above), the dark-state intensity will be zero if the optics do not induce rotation. In general, the dark-state intensity of the ideal light valve will be zero in an optical system if $\text{Re}[e^{-2i\Omega}\vec{P}\cdot\vec{\theta}]=0$. In this case the depolarization $\delta E/E$ at the mirror backplane of the light valve can have a

constant rotation Re[F] that is common to all rays; the remaining ray-dependent portion of the polarization must be purely elliptical. This represents a generalization of the symmetry condition in Figure 8 to the case of any ideal light valve (not necessarily mirrorlike).

4. Light valve is nearly ideal

The crossed-polarizer reflectivity of a dark-state light valve must be small compared to 1 if the light valve is to provide useful performance. For such a light valve we can show that one portion of the single-pass depolarization from the optics will cancel in double pass, while the remaining portion (in quadrature with the first) will double. For a mirrorlike dark state (case 2 above) these portions are, respectively, the ellipticity and rotation, but in general they are defined by a phase relationship involving the light-valve depolarization. The light-valve depolarization also contributes a direct term to the dark state. To derive these results, we rewrite Equation (48) as

$$B = g_{12}^{2} \left\{ 1 + 4 \left(\vec{\theta} \cdot \text{Im} \left[\frac{g_{11}}{g_{12}} \vec{P} \right] \right)^{2} \right\}, \tag{56}$$

where we have made use of the fact that g_{12} is pure real if the active layer of the light valve obeys Equation (8). The quantity g_{11}/g_{12} appearing in Equation (56) can be rewritten as $1/D^*$, where D is the depolarization introduced by the light valve alone; i.e., D is the ratio E_x/E_z when reflected field $\vec{E}_{\text{Reflected}} = (E_x, E_z)$ is produced by illuminating the light valve (at $\vec{\theta} = 0$) with a unit amplitude polarized along \hat{z} . If the light valve provides high contrast, g_{11} will have magnitude close to 1, and to first order we can set $D=g_{12}e^{i\Lambda_{\rm LV}}$, where $\Lambda_{\rm LV}$ is the phase of the light-valve depolarization and g_{12} its magnitude. (Since g_{12} is real, it does not affect the phase of D; $-\Lambda_{LV}$ is the phase of g_{11} .) In the general case where light-valve contrast is not necessarily high, we can set $|g_{11}|^2 = 1$ g_{12}^2 . The single-pass transmission of the optics between crossed polarizers (integrated over NA) is $\langle B_{One-pass} \rangle =$ $|P|^2 NA^2/4$. Defining Λ_{Optics} as the phase of the optics depolarization P, we then have for the double-pass output between crossed polarizers [integrating Equation (56) over

$$\begin{split} \langle \mathbf{B} \rangle &= \mathbf{B}_{\mathrm{LV}} + 4 \langle \mathbf{B}_{\mathrm{One-pass}} \rangle (1 - \mathbf{B}_{\mathrm{LV}}) \, \sin^2 \left(\Lambda_{\mathrm{LV}} + \Delta_{\mathrm{Optics}} \right) \\ &\cong \mathbf{B}_{\mathrm{LV}} + 4 \langle \mathbf{B}_{\mathrm{One-pass}} \rangle \, \sin^2 \left(\Lambda_{\mathrm{LV}} + \Lambda_{\mathrm{Optics}} \right), \end{split} \tag{57}$$

where we have denoted the dark-state reflectivity g_{12}^2 of the light valve alone as $B_{\rm LV}$, and where for simplicity we have assumed telecentric optics, with surface tilts about parallel axes. The upper form of Equation (57) applies in general; the lower form, when the light-valve contrast is large compared to 1. Equation (57) states that when a light valve has reasonably high contrast, part of the single-pass depolarization introduced by the optics will double in the return pass, namely the depolarization that is in

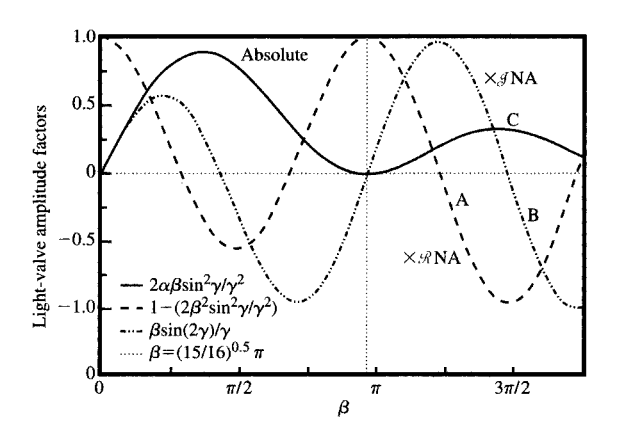


Figure 9

Residual dark-state amplitude for TNLC light valve. [Dark-state is not mirrorlike, except at $\beta = 0.968\pi$ (dotted line).] Amplitude contributions A and B are proportional to NA (intensity $\propto NA^2$), and also respectively to the single-pass rotational and elliptical depolarization induced by the optics. The amplitude component C is independent of NA.

quadrature with the depolarization from the light valve. The doubled amplitude causes a fourfold increase in dark-state intensity, as indicated in Equation (57). The remaining portion of the optics depolarization [of squared magnitude $\langle B_{\text{One-pass}} \rangle \cos^2{(\Delta_{\text{LV}} + \Lambda_{\text{Optics}})}]$ is automatically canceled in double pass. The quadrature relationship is a consequence of the opposite reversal symmetries obeyed by the optics and the active layer of the light valve.

5. Twisted nematic liquid crystal light valve Using Equation (9) to calculate a_1 and a_4 in Equations (41) and (49) [or, alternatively, solving for the parameters in Equation (8)], we find

$$\langle \mathbf{B} \rangle = \left(\frac{2\alpha\beta \sin^2 \gamma}{\gamma^2} \right)^2 + \left(\Re_{\theta} \left[1 - \frac{2\beta^2 \sin^2 \gamma}{\gamma^2} \right] + \Im_{\theta} \left[\frac{\beta \sin (2\gamma)}{\gamma} \right] \right)^2 NA^2 + B_{0, \text{LV}} + B_{0, \text{Optics}},$$
 (58)

where again to shorten the result we have assumed telecentricity and a common tilt axis.

Since Equation (58) represents a case of considerable practical interest, we have added two phenomenological parameters $B_{0,LV}$ and $B_{0,Optics}$ that account for any background contributed by mechanisms outside the models of Equations (9) and (19). ($B_{0,LV}$ refers to such residual background from the light valve, $B_{0,Optics}$ to that from the optics.) The first term in Equation (58) represents the direct depolarization contribution from the light valve; the

light valve also interacts with rotation \Re and ellipticity \Im in the optics via the two terms in square brackets, which then contribute to background $\propto NA^2$.

Figure 9 shows a plot of the three TNLC factors appearing in Equation (58); the g_{12} off-diagonal term, and the two expressions in square brackets which multiply the rotation and ellipticity contributed by the optics.

6. Twisted nematic liquid crystal light valve operating in near-mirror condition

The Jones matrix for the single-pass TN active layer [Equation (6)] reduces to the identity matrix when parameter β (defined by $\beta = \pi d(n_e - n_o)/\lambda$) takes on the value $\sqrt{m^2\pi^2 - \alpha^2}$, with α the twist angle and m a positive integer. The light-valve matrix [Equation (9)] then becomes equivalent to a mirror, and dark-state background is given by $(\Re_{\theta}^2 + \Re_{\phi}^2)NA^2$. We would typically expect this condition to be met at only one wavelength in the spectral illumination band. Taking as an example $\alpha = 45^\circ$, m = 1, we can expand Equation (58) in a small departure $\delta\beta$ from the point of mirrorlike behavior (so that $\delta\beta = \beta - \sqrt{15}\pi/4$), to obtain

$$\langle \mathbf{B} \rangle \cong \left(\frac{15\sqrt{15}\delta\beta^2}{128} \right)^2$$

$$+ NA^2 \left[\Re_{\theta} + \Im_{\theta} \frac{15}{8} \delta\beta + \left(\frac{3\sqrt{15}}{64\pi} \Im_{\theta} - \frac{225}{128} \Re_{\theta} \right) \delta\beta^2 + \cdots \right]^2$$

$$+ \mathbf{B}_{0,\text{Optics}} + \mathbf{B}_{0,\text{SLM}} . \tag{59}$$

If NA and $\delta\beta$ are regarded as first-order quantities, then in lowest order the light valve interacts with the optics in mirrorlike fashion, via the quadratic $\Re^2 NA^2$ term. If rotation \Re and ellipticity \Im are both nonzero, the next-order term is cubic, proportional to $NA^2\delta\beta$ and to $\Re\times\Im$. When rotation is zero, the two lowest-order terms are both quartic, proportional to $NA^2\delta\beta^2$ and to $\delta\beta^4$. Note that unless $\Re=0$, the quadratic and cubic terms involving the optics tend to dominate the g_{12} term that arises from the light valve alone. Unless NA can be regarded as negligible, or the optical system introduces no rotation, there can be a fairly substantial range of wavelengths about $\delta\beta=0$ in which depolarization involving the optics dominates over the contrast measured from the light valve alone.

7. PBS/TNLC module

The most common optical arrangement for reflective light valves is the simple PBS. Light of a particular color is introduced into one port of the beam splitter where it illuminates the light valve (e.g., in reflection, as in Figure 3); light switched to the bright state exits the PBS through a different port. Bleha [27] has published a typical layout. Multiple modules can be used to project different colors, or the colors can be projected sequentially from a single module at a high enough switching speed to appear continuous. Alternatively, a mosaic of (normal-incidence) color filters can be placed on the pixel grid. The common feature in all such approaches is that no tilted coatings other than the PBS hypotenuse see both bright-state and dark-state light.

In such a system $\Im_{\theta} = 0$ (along with \Im_{ψ} , \Re_{ψ}), and $\Re_{\theta} = 1/(n_{\text{PBS}} \tan \Phi)$, where Φ is the angle of incidence at the PBS ($\Phi = 45^{\circ}$ for a cube beam splitter) and n_{PBS} is the refractive index of the PBS substrates. The illumination polarization is rotated but not elliptical. For a TNLC light valve, Equation (58) becomes

$$\langle \mathbf{B} \rangle_{\text{NA}} = \left(\frac{2\alpha\beta \sin^2 \gamma}{\gamma^2} \right)^2 + \left(1 - \frac{2\beta^2 \sin^2 \gamma}{\gamma^2} \right)^2 \frac{NA^2}{n_{\text{PBS}}^2 \tan^2 \Phi} + \mathbf{B}_{0.1\text{V}} + \mathbf{B}_{0.0\text{price}}.$$
 (60)

If the PBS coating is of the usual MacNeille type, the parameters $n_{\rm PBS}$ and Φ are not fully independent, because light must be incident at the interfaces between the lowand high-index layers at the Brewster angle. If we make such Brewster incidence an explicit condition, Equation (60) can be rewritten in various forms:

$$\langle \mathbf{B} \rangle_{\text{NA}} \cong \left(\frac{2\alpha\beta \sin^2 \gamma}{\gamma^2} \right)^2 + \left(1 - \frac{2\beta^2 \sin^2 \gamma}{\gamma^2} \right)^2 \left[\frac{1}{n_{\text{L}}^2} + \frac{1}{n_{\text{H}}^2} - \frac{1}{n_{\text{PBS}}^2} \right] NA^2 + \mathbf{B}_{0,\text{LV}} + \mathbf{B}_{0,\text{Optics}},$$

$$(61)$$

or

$$\langle \mathbf{B} \rangle_{\text{NA}} \cong \left(\frac{2\alpha\beta \sin^2 \gamma}{\gamma^2} \right)^2$$

$$+ \left(1 - \frac{2\beta^2 \sin^2 \gamma}{\gamma^2} \right)^2 \left[\frac{1}{n_{\text{L}}^2} + \frac{1}{n_{\text{H}}^2} \right] \cos^2 \Phi N A^2$$

$$+ \mathbf{B}_{0,\text{LV}} + \mathbf{B}_{0,\text{Optics}}, \qquad (62)$$

where $n_{\rm L}$ and $n_{\rm H}$ are the indices of the low- and high-index materials in the PBS coating.

8. PBS/TNLC module with quarter-wave retarder

We have seen in item 2 above that when the light valve is mirrorlike, ellipticity in the illumination will be canceled out in double pass through the optics; two-pass depolarization arises only from rotation in the illuminating polarization. When the illumination depolarization is pure rotation, as with the PBS/TNLC module in item 7 above, it can be converted to purely elliptical depolarization by placing a quarter-wave retarder on top of the light valve. The waveplate must in the ideal case be oriented so that its retardation axes are rectilinear with the illuminating dark-state polarization of the central ray. The TNLC is likely to be mirrorlike at only a single wavelength in the band; when we apply Equation (58) in the case of pure ellipticity from a PBS and 90° retarder, we find that for other wavelengths,

$$\langle \mathbf{B} \rangle_{\text{NA}} = \left(\frac{2\alpha\beta \sin^2 \gamma}{\gamma^2} \right)^2 + \left(\frac{\beta \sin (2\gamma)}{\gamma} \right)^2 \frac{NA^2}{n_{\text{PBS}}^2 \tan^2 \Phi} + \mathbf{B}_{0.\text{LV}} + \mathbf{B}_{0.\text{Optics}}.$$
 (63)

The difference between Equation (60) and Equation (63) is in the two LC factors that multiply the optics factor $NA^2/(n_{PBS}^2 \tan^2 \Phi)$. These are two of the curves plotted in Figure 9; without the waveplate, the interaction depolarization is largest in the center of the band, whereas with the waveplate, contrast loss is eliminated at the center of the band (where the light valve is mirrorlike). At other wavelengths the dark-state background with the quarter-wave retarder remains larger than the g_{12}^2 term contributed by the light valve alone. Even with the waveplate in place, the quadratic interaction term is still the dominant source of contrast loss near the center of the band, where the light-valve term is quartic in $\Delta \lambda$. (Of course, all contrast losses are small in this regime.) It should also be noted that Equation (63) assumes an achromatic quarter-wave plate; the dispersion that would be present in a simple single-layer retarder is neglected for simplicity.

9. Light valve rotated under polarizing microscope
The field of view in a microscope is small enough that in a reflection-mode instrument designed for polarization work, the beam can be expanded through the beam splitter in an almost collimated condition; then NA is ~ 0 and compound-angle effects are avoided. The intensity measured between crossed polarizers in such an instrument is simply g_{12}^2 . In a sense, Equation (52) is a generalization of this simple result to include compound-

angle effects at finite NA, but we can generalize it in another way, by calculating residual dark-state intensity as a function of light-valve orientation. [Of course, Equation (52) also applies to a rotated light valve if the active layer is modified by a rotation matrix.]

As in the case of Equation (52), we impose only one constraint on the light-valve matrix $[(g_{11}, g_{12}), (g_{21}, g_{22})]$, namely that it arise from a nonabsorbing active layer (or a layer with equal absorption in the two polarizations) placed above a mirror backplane. Such an active layer must satisfy Equation (8) above; if in its nominal orientation ($\Theta = 0$) the active layer matrix is parametrized according to the second form in Equation (8), then we find using rotation matrices and some algebra that the reflectance measured between crossed polarizers when the active layer is rotated to a new orientation Θ is given by

$$R(\Theta) = R_0 \cos^2 [2(\Theta - \Theta_0)] + B_{0,LV}$$

= $R_0 \sin^2 [2\Theta'] + B_{0,LV}$, (64)

where $B_{0,LV}$ is the same parameter that appears in Equation (58), and where

$$R_0 = 1 - (\sin^2 \mu \cos 2\vartheta + \cos^2 \mu \cos 2\zeta)^2, \tag{65}$$

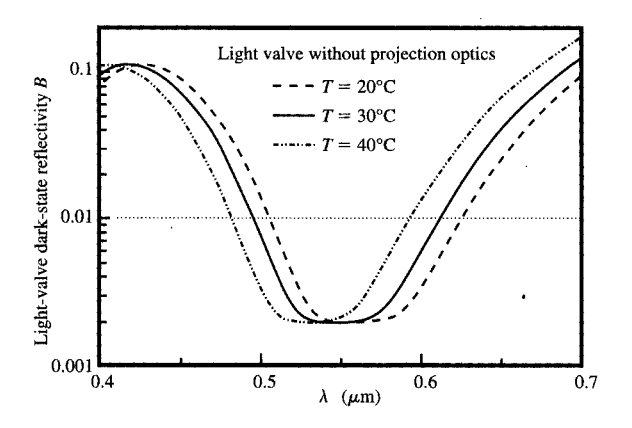
and

$$\tan 2\Theta_{\theta} = \frac{\cos(\vartheta + \zeta)}{\tan 2\mu} - \frac{\sin(\vartheta + \zeta)}{\tan(\vartheta - \zeta)\sin 2\mu},\tag{66}$$

and where $\Theta' \equiv \Theta - [\Theta_0 - (2m + 1)\pi/4]$, with m an integer.

According to Equation (64), the observation of a harmonic intensity variation (having 90° period) when a reflective light valve is rotated between crossed polarizers is generic, and in itself conveys little information about the properties of the light valve; however, quantitative measurements of the angle of maximum reflectivity Θ_0 and the maximum reflectivity value R_0 suffice to constrain the active layer in two of the three degrees of freedom permitted by Equation (8). The $\cos^2(2\Theta)$ modulation will be zero in all orientations only if $R_0 = 0$ (in which case it follows form Equations (8) and (65) that the active layer must be either null, equivalent to a half-wave retarder, or equivalent to a pure rotation (optically active layer), but in the ideal case where $B_{0,LV} = 0$, the reflectance between crossed polarizers will always have a zero at $\Theta = \Theta_0 + \pi/4$. Because $\Theta = 0$ corresponds to the normal orientation of the light valve, it may be convenient to shift the angular coordinate system according to the lower form of Equation (64), since contrast is likely be high at small values of Θ.

10. TNLC light valve rotated under polarizing microscope In the particular case of a TNLC light valve [as in Equation (9), single-pass active layer as in Equation (6)],



Variation of TN light-valve dark state with wavelength and temperature, in low-NA optical system. Incoherent background is 0.002. LC dispersion is for a commercially available liquid crystal material.

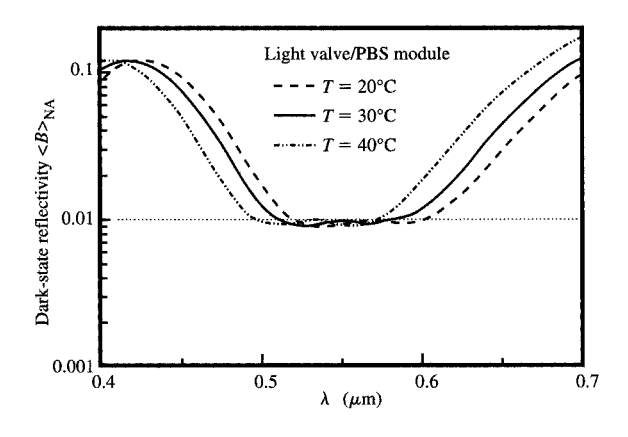


Figure 11

TN light-valve dark state as projected through PBS. Optics contribute 0.002 incoherent background. NA is 0.143 (f/3.5) and $n_{\rm PBS}$ is 1.85.

Equation (64) becomes

$$R(\Theta) = R_0 \sin^2 \left[2(\Theta - \Theta_0') \right] + B_{0,LV},$$
 (67)

with

$$R_0 = \left(\frac{2\beta \sin \gamma}{\gamma}\right)^2 \left(1 - \left[\frac{\beta \sin \gamma}{\gamma}\right]^2\right)$$

and

$$\tan 2\Theta_0' = \frac{\alpha \tan \gamma}{\gamma}. \tag{68}$$

Discussion

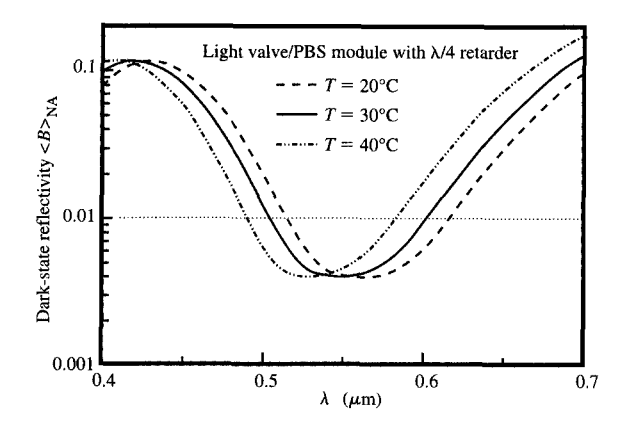
We now discuss some implications of the results of the previous section. Figure 10 plots Equation (64) (at $\Theta = 0$) as a function of λ , for a TNLC active layer [Equations (67) and (68)], using $\Delta n[\lambda]$ values for a commercially available liquid crystal material. The parameter α is set to $\pi/4$. The curve of Figure 10 is the spectral response of the light valve if measured between crossed polarizers using a polarizing microscope (see also below). Figure 10 can also be regarded as an application of the curve of Figure 6 to a particular LC layer. The LC thickness is chosen such that when temperature $T = 30^{\circ}$ C, parameter y becomes equal to π at $\lambda = 545$ nm; 545 nm is then the nominal wavelength of maximum contrast. $\Delta n \equiv n_a - n_a$ is about 0.2 at this wavelength, and the required LC thickness is 2.64 μ m. $\lambda = 545$ nm might, for example, be the center of a green channel extending from 515 nm to 575 nm. For the sake of illustration we have set $B_{0.1V} = 0.002$. The change in $n_c - n_a$ with temperature is roughly -0.35%per °C. (A slightly more detailed T dependence is used in the plots.) The spectral dispersion in $n_c - n_o$ is roughly -0.5% per 1% increase in λ .

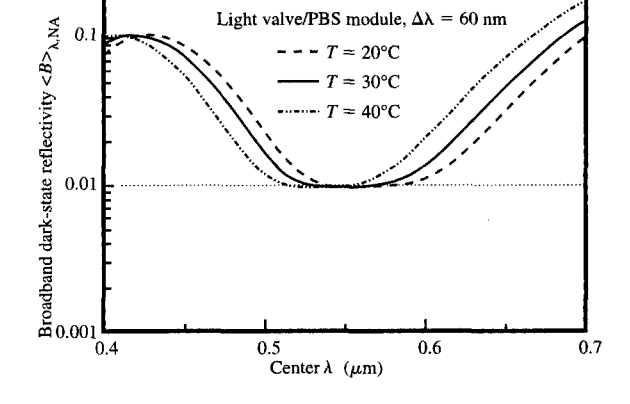
All curves in Figure 10 are essentially equivalent to the curve in Figure 6, with a different mapping of parameter β onto λ for each temperature. Since $\beta \equiv \pi (n_e - n_o) d/\lambda$, a pair of balancing shifts ΔT and $\Delta \lambda$ that hold β at some constant value (e.g., the value $(\sqrt{15}/4)\pi$ associated with the minimum of the curve) must be related by

$$\frac{1}{\lambda_0} \frac{\Delta \lambda}{\Delta T} \simeq -\frac{1}{\lambda_0} \frac{\partial \beta / \partial T}{\partial \beta / \partial \lambda} = -\frac{\partial (\ln [\Delta n]) / \partial T}{\partial (\ln [\Delta n/\lambda]) / \partial (\ln \lambda)}.$$
 (69)

If Δn changes by 0.35% per °C, and $\Delta n/\lambda$ by 1.5% per 1% change in λ , then Equation (69) predicts a 0.23% shift in minimum wavelength per °C. The curves of Figure 10 shift with temperature at about this rate. At a fixed 30°C temperature, the range of wavelengths where background is below 0.01 is 115 nm; however, it is only over a smaller 85-nm-wavelength range that background is below 0.01 at all temperatures between 20°C and 40°C. A 30-nm contraction of the tolerance window over 20°C at $\lambda = 545$ nm is approximately what would be expected from the linear approximation in Equation (69).

We next consider the effect of the optical system. Figure 11 plots the system background when the light valve of Figure 10 is used with a basic PBS/TNLC module [Equation (60)]. The calculation uses $n_{\rm PBS}=1.85$ and NA=0.143 (f/3.5 optics). Figure 12 plots the example of Figure 10 with a quarter-wave retarder placed over the TNLC light valve [Equation (63)], also for the case $n_{\rm PBS}=1.85$ and NA=0.143. In both cases a constant scatter background from the optics $B_{0,{\rm Optics}}=0.002$ is assumed for purposes of illustration. Over small changes in temperature and wavelength, the dark-state intensity





Same conditions as Figure 11, but $\lambda/4$ retarder is placed above light valve to improve contrast.

Figure 10

Same conditions as Figure 11, but averaged over $\Delta\lambda=60$ nm bandwidth.

in Figure 11 is dominated by the constant $\Re^2 NA^2$ background that the PBS would produce if the light valve were perfectly mirrorlike. When a quarter-wave retarder is added, as in Figure 12, the background level at fixed NA has a quadratic variation with wavelength over much of the plotted region.

Figures 11 and 12 are essentially plots of (contrast)⁻¹ versus wavelength for a TNLC light valve whose dark state is mirrorlike at $\lambda = 545$ nm. (Strictly speaking, contrast can be identified as the reciprocal of (B) only if dark-state and bright-state efficiencies are equal.) Figures 13 and 14 show integrals over a spectral range $\Delta \lambda = 60$ nm of the curves of Figures 11 and 12; the horizontal axis in Figures 13 and 14 is the center wavelength λ_0 of the integration band. In a sense, Figures 13 and 14 could be regarded as plots of integrated contrast in a color channel having 60-nm bandwidth. These integrations are somewhat artificial, because the mean wavelength of the color channel is shifted without regard for chromaticity requirements, but the curves of Figures 13 and 14 are roughly equivalent to plots of \(\lambda\)-averaged background as a function of LC thickness d, if due allowance is made for the dispersion of Δn . The finite-wavelength band always degrades contrast slightly in the region of interest; the degradation can be regarded as a larger relative effect in the case of Figure 14 with quarter-wave retarders, because the total background is lower.

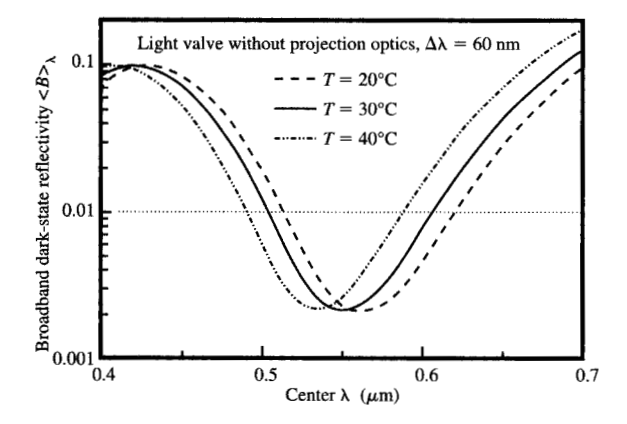
The analysis of the preceding sections allows contrast to be calculated for a particular optical system of interest, but there are general trends that can be noted if further simplifications are made. First, if we regard the NA, the relative bandwidth $\Delta\lambda/\lambda_0$, and the fractional cell-gap error

Flaure 1

Same conditions as Figure 12, but averaged over $\Delta \lambda = 60$ nm bandwidth.

 $\Delta d/d$ (including the effective change in cell gap due to temperature excursion) as first-order quantities, then Equation (59) above shows that the lowest-order background term arises from rotation in the illuminating polarization (causing background B $\sim \Re^2 NA^2$). For the PBS/TNLC module without quarter-wave plates, we can therefore say as a rough approximation that, for $\Delta \lambda/\lambda_0$ and $\Delta d/d$ small, background is approximately

$$B \approx B_{0,LV} + B_{0,Optics} + \frac{NA^2}{n_{PBS}^2 \tan^2 \Phi}.$$
 (70)



Same conditions as Figure 10, but averaged over $\Delta \lambda = 60$ nm bandwidth. Comparison with Figures 13 and 14 shows the narrowing of light-valve LC thickness tolerances due to interaction with the optical system.

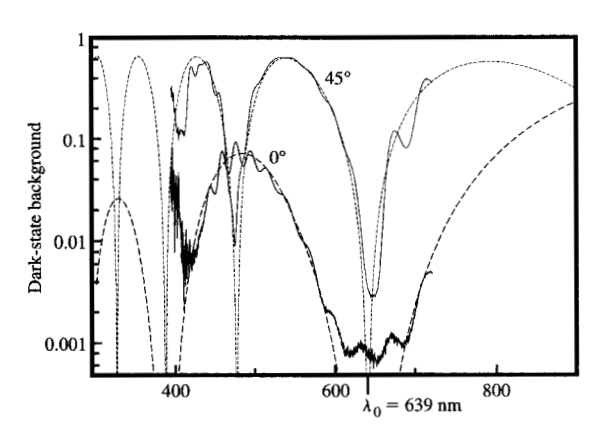


Figure 16

Multiple reflections within TNLC layer give rise to Fabry-Perot oscillations in the reflected spectrum. Fits to the spectra based on a single-round-trip model can be used to establish the LC thickness, allowing prediction of contrast in an optical system. The figure shows crossed-polarizer spectra taken in two different orientations of the light valve, along with fitted curves [obtained from Equations (67) and (68)].

If $\Phi = 45^{\circ}$ and $n_{PBS} \cong 1.7$, we then have as a rough scaling rule

$$B \sim B_{0,LV} + B_{0,Optics} + \frac{NA^2}{3}$$
 (71)

Equation (71) is highly simplified, but it suggests that a

typical requirement of contrast \gtrsim 100:1 limits NA to \sim 0.15 for a PBS/TNLC module operating without quarter-wave retarder.

The case in which a quarter-wave retarder is added to the module (item 8 above) is somewhat more complicated. An expansion along the lines of Equation (59) contains a number of lowest-order (quartic) terms; the essential action of the retarder is in effect to subtract the lowest-order (quadratic) term represented by Equation (70). The fully general expression in Equation (63) is fairly simple, but becomes more complicated when expressed in terms of the underlying physical parameters d, $\Delta n(\lambda, T)$, and λ . To obtain a simplified result, we expand β in terms of a small shift $\delta\lambda$ away from the central wavelength λ_0 , a small temperature excursion ΔT , and a small departure Δd of LC thickness from nominal:

$$\beta[\lambda + \delta\lambda] \cong \pi \sqrt{1 - W^2} \left(1 + \mathbb{K} \frac{\delta\lambda}{\lambda_0} + \frac{\delta\beta_0}{\beta_0} \right), \tag{72}$$

where

$$\mathbb{K} = \frac{\partial \ln \left(\frac{\Delta n(\lambda, T)}{\lambda} \right)}{\partial \ln \lambda} \bigg|_{\lambda = \lambda_0} . \tag{73}$$

Parameter W is defined by $W \equiv \alpha/\pi$, and the systematic fractional offset in β is defined by

$$\frac{\delta \beta_0}{\beta_0} = \frac{\Delta d}{d} + \Delta T \frac{\partial \ln (\Delta n)}{\partial T}.$$
 (74)

We approximate Equation (63) under the assumption that the background intensity of interest is the average of B over all wavelengths present in a particular color channel (as well as over NA); the spectral extent $\Delta\lambda$ of the color channel is defined by $\lambda_0 - (\Delta\lambda/2) \le \lambda_0 + \delta\lambda \le \lambda_0 + (\Delta\lambda/2)$. We would like to estimate the integrated channel background as a function of channel bandwidth $\Delta\lambda$, LC error $\delta\beta_0/\beta_0$, and NA. In general the channel spectrum has some distribution $P(\lambda)$, which may include a lumen-weighting factor representing the eye's efficiency. For a flat spectrum [i.e., $P(\lambda) = 1$], the average over the *m*th power in a spectral expansion is given by

$$\left\langle \left(\frac{\delta\lambda}{\lambda_0}\right)^m\right\rangle_{\lambda} = \frac{1}{\lambda_0^m} \frac{\int_{-\Delta\lambda/2}^{+\Delta\lambda/2} (\delta\lambda)^m d\lambda}{\int_{-\Delta\lambda/2}^{+\Delta\lambda/2} d\lambda}$$

$$= \begin{cases} \frac{1}{2^m (m+1)} \left(\frac{\Delta\lambda}{\lambda_0}\right)^m & m \text{ even,} \\ 0 & m \text{ odd.} \end{cases}$$
(75)

For m = 2, the flat spectrum average of $(\delta \lambda/\lambda)^2$ from

A. E. ROSENBLUTH ET AL.

Equation (75) is $(1/12)(\Delta\lambda/\lambda)^2$, where $\Delta\lambda$ is the full width of the channel. For the more general case where $P(\lambda)$ is not constant, we then define an effective channel width $(\Delta\lambda/\lambda_0)_{\rm eff}$ according to

$$\left(\frac{\Delta\lambda}{\lambda_0}\right)_{\text{eff}} = \frac{1}{\lambda_0} \sqrt{12 \frac{\int_{-\Delta\lambda/2}^{+\Delta\lambda/2} P(\lambda_0 + \delta\lambda)(\delta\lambda)^2 d\lambda}{\int_{-\Delta\lambda/2}^{+\Delta\lambda/2} P(\lambda_0 + \delta\lambda) d\lambda}}.$$
(76)

For simplicity we further assume that the average of $(\delta\lambda/\lambda)^4$ is equal to $(1/80)(\Delta\lambda/\lambda_0)_{\rm eff}^4$, even though according to Equation (75) this is only strictly true for a flat spectrum. We similarly make the approximation that the average of any odd power of $(\delta\lambda/\lambda)$ is negligible, even with a nonconstant spectrum. Dispersion in the retarder is also neglected.

Keeping only the lowest-order terms in Equation (63), we find

Figure 15 shows the result of integrating with respect to
$$\lambda$$
 the curve of Figure 10 for the background contribution of the light valve alone; the range of integration is the same as in Figures 13 and 14. Comparison of Figures 13, 14, and 15 illustrates the narrowing of light-valve LC thickness tolerances due to interaction with the optical system.

The incoherent contribution from the optics, $B_{0,\text{Optics}}$, can be measured by replacing the light valve in the PBS/TNLC module with a mirror (leaving the quarter-wave retarder in place). Because of the interaction term in Equation (63), it is not accurate to calculate system contrast by simply adding to $B_{0,\text{Optics}}$ the contribution of the light valve as measured with a polarizing microscope. Instead, more extensive light-valve measurements must be made in order to determine the thickness d of the LC active layer as fabricated (including possible thickness variation over the active area), and the incoherent background term $B_{0,\text{LV}}$. We have described our measurement procedure and apparatus elsewhere [28, 29]. **Figure 16** illustrates one

$$\langle \mathbf{B} \rangle_{\lambda, \mathrm{NA}} \approx 4 \pi^{2} (1 - W^{2})^{3} \left\{ \pi^{2} W^{2} (1 - W^{2})^{2} \left[\frac{\mathbb{K}^{4}}{80} \left(\frac{\Delta \lambda}{\lambda} \right)_{\mathrm{eff}}^{4} + \frac{\mathbb{K}^{2}}{2} \left(\frac{\Delta \lambda}{\lambda} \right)_{\mathrm{eff}}^{2} \left(\frac{\delta \beta_{0}}{\beta_{0}} \right)^{2} + \left(\frac{\delta \beta_{0}}{\beta_{0}} \right)^{4} \right] \right.$$

$$\left. + \frac{NA^{2}}{n_{\mathrm{PBS}}^{2} \tan^{2} \Phi} \left[\frac{\mathbb{K}^{2}}{12} \left(\frac{\Delta \lambda}{\lambda} \right)_{\mathrm{eff}}^{2} + \left(\frac{\delta \beta_{0}}{\beta_{0}} \right)^{2} \right] \right\} + \mathbf{B}_{0, \mathrm{LV}} + \mathbf{B}_{0, \mathrm{Optics}}. \tag{77}$$

The coefficients in Equation (77) that multiply powers of the systematic error $(\delta\beta/\beta)$ tend to be somewhat larger than those multiplying powers of the bandwidth $(\Delta\lambda/\lambda)_{\rm eff}$. Image brightness increases as spectral bandwidth increases, but chromaticity considerations prevent bandwidth $(\Delta\lambda/\lambda)_{\rm eff}$ from exceeding ~ 0.12 to 0.18 in a single color channel. Image brightness also increases with increasing NA; however, besides lowering contrast, practical considerations such as lens cost and component size also limit NA in this type of projector.

To simplify Equation (77) still further, we assume that at the practical limit, $NA \sim 0.25$ and $(\Delta \lambda/\lambda)_{\rm eff} \sim 0.15$. For $\mathbb{K} \sim 1.5$ and W = 0.25, we find from Equation (77) that the quartic terms in cell-gap error are fairly small, and that

$$\langle \mathbf{B} \rangle_{\text{A,NA}} \sim \mathbf{B}_{0,\text{LV}} + \mathbf{B}_{0,\text{Optics}} + 0.0035 + 1.1 \left(\frac{\delta \beta_0}{\beta_0} \right)^2. \tag{78}$$

Equation (78) is of course very rough, but it suggests that when a quarter-wave retarder is combined with a PBS/TNLC module in a projector with $\sim \! 100:\! 1$ contrast target, compound-angle depolarization will not be the dominant factor limiting the NA as long as cell-gap errors (and equivalent temperature excursions) are held to $\sim \! 5\%$. When we consider depolarization from the light valve alone, we obtain tolerances that are $\sim \! 50\%$ more relaxed.

complication that is seen in experimental data. The solid curve shows measured reflectivity as a function of λ for a TNLC light valve between crossed polarizers, at NA=0.2. The ripple structure is due to interference across the TNLC layer. Yang and Takano have analyzed this phenomenon in detail as a multiray Fabry-Perot interference across a dispersive TN medium [30]. The dashed curves in Figure 16 are fittings of Equations (67) and (68) to the spectrum, which we use to determine the LC thickness d. We obtain reasonably consistent results with this method, even though Equation (67) neglects multiple reflections within the LC layer.

Summary

Projectors that use reflective light valves must employ beam splitters or analogous components to separate bright-state light from dark-state light. With transmissive light valves, this function can be carried out by a simple sheet post-polarizer which trims dark-state light from the bright-state image beam. However, when the light valve is reflective, both states must be allowed to propagate in the space above the substrate, and the beam-splitter element (PBS) must actually separate the two beams.

Beam-dividing interference coatings give rise to polarization crosstalk via compound-angle depolarization,

as illustrated in Figure 3 for a PBS coating. Other tilted coatings in the projection optics may also contribute to this depolarization, as illustrated in Figure 4. The depolarization gives rise to undesired intensity in the dark-stage image, causing contrast to degrade proportional to NA^{-2} . The unwanted background has the same polarization as the bright-state image and cannot be filtered out with a supplementary polarizer.

In Equations (19)–(22) we have presented a solution for the depolarization arising in a general optical system, retaining terms in the depolarization amplitude proportional to NA ($\propto NA^2$ in intensity). Good agreement has been found with exact numerical polarization ray tracing [using Equations (10) and (11)] when $NA \leq 0.14$ (i.e., for apertures below $\sim f/3.5$). Our solution applies to any assembly of tilted coatings, so long as 1) all surfaces are tilted in such a way that the polarization of the central ray is either pure S or pure P (i.e., the optical system introduces no deliberate depolarization), and 2) none of the tilted optical coatings through which the beam passes in transmission are deposited on tilted refractive wedges (which if used would cause severe aberration of the beam). The solution applies to systems employing tiltedplane parallel substrates (such as plate dichroic filters or plane parallel tilted air spaces), as well as TIR reflections or tilted internal coatings like that in a PBS cube.

We have reviewed the Jones-matrix theory of reflective twisted nematic liquid crystal (TNLC) light valves, and have noted that the dark state in such light valves is exactly mirrorlike only at isolated wavelengths, typically at only a single wavelength in the operating spectral range. We have shown that to avoid contrast loss from the compound-angle depolarization mechanism when the light valve is mirrorlike, the optical system must not induce any rotation in the polarization of skew rays illuminating the light valve. On the other hand, ellipticity induced in the illumination will automatically be canceled out in the return pass through the optics. Pure rotation in the illuminating light can be converted to pure ellipticity by placing a quarter-wave retarder on top of the light valve.

This rule for depolarization of skew rays by projection optics is opposite to what is required of the light-valve active layer itself: In dark state the active layer of a reflective light valve should not introduce ellipticity in the polarization of the central ray (when the ray reaches the mirror backplane); on the other hand, any rotation of polarization that it might introduce will be canceled out in the return pass through the active layer.

At most wavelengths, TNLC light valves in dark state do not behave exactly as mirrors. We have derived in Equation (58) an expression for their contrast loss in an optical system which induces both ellipticity and rotation in the illuminating polarization. Equation (52) generalizes further, presenting the solution for a general polarizationmodulating light valve in a general optical system. Equation (52) and the first form of Equation (57) apply to any reflective light valve whose active layer is lossless (or has equal attenuation in the two polarizations). Dark-state intensity of such a light valve in a projector increases with the square of the angular extents of the beam, i.e. for an aligned and telecentric system, as NA^2 .

Finally, the second form in Equation (57) applies whenever the light-valve contrast is large compared to 1 (the case of primary practical importance). Equation (57) shows that one part of the single-pass depolarization introduced by the optics is canceled in the second pass that follows reflection from the light valve, while the remaining portion is doubled (in amplitude, quadrupled in intensity). The portion that is doubled over the round trip is the portion in quadrature with the light-valve depolarization. (This portion is the rotational depolarization when the light valve is mirrorlike.)

The case of a TNLC light valve interacting with a simple PBS optical system has been explored in some detail, both with and without an added quarter-wave retarder to improve contrast. With no quarter-wave retarder, a rule of thumb is that the dark-state background can be estimated as $B \approx NA^2/n_{PBS}^2 \sim NA^2/3$ [see Equations (70) and (71)].

Acknowledgments

The authors gratefully acknowledge the help of Steve Lovas in fabricating light valves and optical components used in this study. We also thank Hideo Kawakita and Kunio Enami of IBM Japan for many helpful discussions.

References

- J. Glueck, E. Ginter, E. Lueder, and T. Kallfass, "Reflective TFT-Addressed LC Light-Valve Projectors with High Light Efficiency," Digest of Technical Papers, Society for Information Display International Symposium, Richard H. Bruce and Hugo Steemers, Eds., 1995, p. 235.
- J. Bowron and T. Schmidt, "A New High Resolution Reflective Light Valve Projector," to be published in Projection Displays IV, Proc. SPIE 3296, M. H. Wu, Ed. (1998).
- F. E. Doany, R. N. Singh, A. E. Rosenbluth, and G. L.-T. Chiu, "Projection Display Throughput: Efficiency of Optical Transmission and Light-Source Collection," *IBM J. Res. Develop.* 42, 387–399 (1998, this issue).
- M. Imai, M. Sakamoto, K. Kubota, Y. Kato, and N. Nishida, "High-Brightness Liquid Crystal Light Valve Projector Using a New Polarization Converter," *Large* Screen Projection Displays II, Proc. SPIE 1255, 52 (1990).
- M. S. Brennesholtz, "Light Collection Efficiency for Light Valve Projection Systems," Projection Displays II, Proc. SPIE 2650, 71 (1996).
- R. M. Knox and J. R. Masters, "Extra-Folded Projection Display System Including a Linear Reflective Polarizer Placed Immediately Behind the System's Imaging Screen," European Patent EP 783,133, 1997.

- D. L. Wortman, "A Recent Advance in Reflective Polarizer Technology," *Proceedings of the 1997 International Display Research Conference* (Society for Information Display), 1997, p. M-98.
- for Information Display), 1997, p. M-98.

 8. R. Maurer and D. Andrejewski, "Polarizing Color Filters Made from Cholesteric LC Silicones," Digest of Technical Papers, Society for Information Display International Symposium, H. Funk and P. Alt, Eds., 1995, pp. 110-113.
- 9. A. J. S. M. DeVaan, "Image Projection System," U.S. Patent 5,573,324, 1994.
- Y. Miyatake, "Polarizing Beamsplitter Apparatus and Lightvalve Image Projection System," European Patent EP 389,240, 1990.
- E. Waluschka, "A Polarization Ray Trace," Opt. Eng. 28, 86-89 (1989).
- S.-T. Wu, "Liquid Crystals," Handbook of Optics, M. Bass, Ed., McGraw-Hill Book Co., Inc., New York, 1995, p. 14.1.
- 13. M. Schadt, "Liquid Crystal Materials and Liquid Crystal Displays," Ann. Rev. Mater. Sci. 27, 305 (1997).
- K. Lu and B. E. Saleh, "Complex Amplitude Reflectance of the Liquid Crystal Light Valve," Appl. Opt. 30, 2354 (1991).
- H. L. Ong, "Origin and Characteristics of the Optical Properties of General Twisted Nematic Liquid-Crystal Displays," J. Appl. Phys. 64, 614 (1988).
- 16. M. C. Mauguin, Bull. Soc. Franc. Miner. Crist. 34, 71 (1911).
- M. Schadt and W. Helfrich, "Voltage-Dependent Optical Activity of a Twisted Nematic Liquid Crystal," Appl. Phys. Lett. 18, 127 (1971).
- C. H. Gooch and H. A. Tarry, "The Optical Properties of Twisted Nematic Liquid Crystal Structures with Twist Angles ≤ 90 Degrees," J. Phys. D 8, 1575 (1975).
- A. Yariv and P. Yeh, Optical Waves in Crystals, Wiley, New York, 1984.
- E. Merzbacher, Quantum Mechanics, Wiley, New York, 1970.
- A. Lien, "Optimization of the Off-States for Single Layer and Double Layer General Twisted Nematic Liquid Crystal Displays," *IEEE Trans. Electron Devices* 36, 1910 (1989).
- N. C. Pistoni, "Simplified Approach to the Jones Calculus in Retracing Optical Circuits," Appl. Opt. 34, 7870–7876 (1995).
- J. Grinberg, A. Jacobsen, W. Bleha, L. Miller, L. Fraas,
 D. Boswell, and G. Myer, "A New Real-Time Non-Coherent to Coherent Light Image Converter: The Hybrid Field Effect Liquid Crystal Light Valve," Opt. Eng. 14, 217–225 (1975).
- 24. K. H. Yang and M. Lu, "Nematic LC Modes and LC Phase Gratings for Reflective Spatial Light Modulators," IBM J. Res. Develop. 42, 401-410 (1998, this issue).
- A. V. Tikhonravov, "Some Theoretical Aspects of Thin-Film Optics and Their Application," Appl. Opt. 32, 5417 (1993).
- A. Thelen, Design of Optical Interference Coatings, McGraw-Hill Book Co., Inc., New York, 1989.
- W. P. Bleha, "Development of ILA® Projectors for Large Screen Display," *Proceedings of the 1995 International Display Research Conference* (Society for Information Display), 1995, p. 91.
- D. B. Dove and A. E. Rosenbluth, "Measurement of the Optical Properties of High Resolution TN-LC Lightvalves," Proceedings of the 1997 International Display Research Conference (Society for Information Display), 1997, p. 105.
- A. E. Rosenbluth, D. B. Dove, and F. Doany, "Contrast Losses in Projection Displays from Depolarization by Tilted Beam Splitter Coatings," *Ibid.*, p. 226.
- Tilted Beam Splitter Coatings," *Ibid.*, p. 226.

 30. K. H. Yang and H. Takano, "Measurements of Twisted Nematic Cell Gap by Spectral and Split-Beam Interferometric Methods," *J. Appl. Phys.* 67, 5-9 (1989).

Received April 21, 1997; accepted for publication February 10, 1998

Alan E. Rosenbluth IBM Research Division, Thomas J. Watson Research Center, P.O. Box 218, Yorktown Heights, New York 10598 (aerosen@us.ibm.com). Dr. Rosenbluth received the Ph.D. degree in optics from the University of Rochester in 1982 as a Hertz Foundation Fellow. He has been a Research Staff Member at the IBM Thomas J. Watson Research Center since 1982. His principal research activities have been in photolithographic instrumentation and processing, display technology, and thin-film optics.

Derek B. Dove IBM Research Division, Thomas J. Watson Research Center, P.O. Box 218, Yorktown Heights, New York 10598 (dove@us.ibm.com). Dr. Dove attended the Imperial College of Science and Technology, London, England, receiving the Ph.D. degree in 1956. After working at AERE, Harwell, for several years, he joined Bell Telephone Laboratories, Murray Hill, New Jersey, where he was involved in studies on the structure and properties of magnetic films. In 1967 he became professor of Materials Science and Electrical Engineering at the University of Florida. In 1977, Dr. Dove joined IBM at Yorktown Heights as a manager in the display and printing area, where he worked on resistive ribbon printing and on electrophotography. More recently, he has worked on phase-shift masks and on optical systems for high-resolution displays.

Fuad E. Doany IBM Research Division, Thomas J. Watson Research Center, P.O. Box 218, Yorktown Heights, New York 10598 (doany@us.ibm.com). Dr. Doany is a Research Staff Member in the Optical Systems group at the IBM Thomas J. Watson Research Center. He received a B.S. degree in chemistry from Haverford College in 1978 and a Ph.D. degree in physical chemistry from the University of Pennsylvania in 1984. Dr. Doany was a Postdoctoral Fellow at the California Institute of Technology from 1984 to 1985, working on ultrafast laser spectroscopy. He subsequently joined IBM at the Watson Research Center, where he worked on laser spectroscopy, laser material processing, and applied optics. His current research activity is in projection display technology. Dr. Doany has written many technical papers, holds more than 15 patents, and has received two Research Division Awards from IBM, in 1994 and 1996. He is a member of the Optical Society of America and the Society for Information Display.

Rama N. Singh IBM Research Division, Thomas J. Watson Research Center, P.O. Box 218, Yorktown Heights, New York 10598 (rsingh@us.ibm.com). Dr. Singh received an M.S. degree in physics from Lucknow University, India, in 1964, a Diploma of the IIT, Delhi, in applied optics in 1966, a Diploma of the Imperial College, London, in applied optics in 1968, a Ph.D. in physics from the University of Reading in the U.K. in 1977, and an M.S. in computer science from Polytechnic University in 1995. Dr. Singh was a member of the faculty of physics at the Indian Institute of Technology, Delhi, until 1980, a principal scientist in the Microlithography Division at Perkin-Elmer from 1980 to 1988, and a Research Staff Member at the IBM Thomas J. Watson Research Center since 1988. His principal interests have been in optical design in the fields of photolithographic instrumentation and display technology.

Kei-Hsiung Yang (K. H. Yang) IBM Research Division, Thomas J. Watson Research Center, P.O. Box 218, Yorktown Heights, New York 10598 (kyang@us.ibm.com). Dr. Yang received his B.S. in physics from the National Taiwan University, his M.S. from the University of Notre Dame, and his Ph.D. from the University of California at Berkeley in 1974. He joined the IBM Thomas J. Watson Research Center in 1979 as a Reseach Staff Member; his work in LCD research has included wide-viewing-angle technologies for TFT/LCD, Si-wafer-based LCLVs for reflective projection displays and holographic optical storage, ferroelectric LC devices, TN electro-optics, LC-to-surface anchoring properties, and the transport properties of LC cells. In 1987, he worked at Toshiba Development Laboratories at Shin-Sugita, Japan, for three months as a member of the IBM-Toshiba TFT/LCD joint development team. Prior to joining IBM, Dr. Yang worked at the General Electric R&D Center (1973-1979) in Schenectady, New York; at the Bell Telephone Laboratories (1969) in Murray Hill, New Jersey: and at the Lawrence Livermore Laboratories (1969-1973) in Berkeley, California. Dr. Yang has received a GE Centennial Patent Award, four IBM Invention Achievement Awards, and an IBM Research Division Group Award. He has 16 U.S. patents and nine patents pending, and more than 50 publications in the field of liquid crystal devices, electrophoretic displays, VUV-fluorescent solids, X-ray imagers for breast cancer diagnosis, and nonlinear optics. Dr. Yang is a member of SID and SPIE.

Minhua Lu IBM Research Division, Thomas J. Watson Research Center, P.O. Box 218, Yorktown Heights, New York 10598 (minhua@us.ibm.com). Dr. Lu received a B.S. in physics from the University of Science and Technology of China (1984), an M.S. in materials science from the Chinese Academy of Sciences (1987), an M.S. in physics from Case Western Reserve University (1990), and a Ph.D. in physics from Case Western Reserve University (1992). She joined the IBM Thomas J. Watson Research Center in 1995 as a Research Staff Member and has been working on Siwafer-based LCLVs for reflective projection displays and holographic optical storage. Prior to joining IBM, she worked for two years as an R&D manager at Kent Display Systems, Kent, Ohio, and for more than half a year as a Postdoctoral Fellow at the Liquid Crystal Institute of Kent State University. She has three U.S. patents and four patents pending, and more than 15 publications in the fields of reflective TN LC devices, fast-switching surface-stabilized cholesteric LCDs including driving, material, and process, polymer-dispersed LC for AMLCDs, and the usage of light scattering to study the polarization and elastic properties of ferroelectric LC and the formation of phospholipid tubules. She is a member of SID and SPIE.